PHYSICAL REVIEW D **94,** 103513 (2016)

General relativistic polytropes with a repulsive cosmological constant

Zdeněk Stuchlík,[*] Stanislav Hledík,[†] and Jan Novotný[‡]
Institute of Physics, Faculty of Philosophy and Science, Silesian University in Opava, Bezručovo nám. 13, CZ-746 01 Opava, Czech Republic
(Received 8 July 2016; published 14 November 2016)

Spherically symmetric equilibrium configurations of perfect fluid obeying a polytropic equation of state are studied in spacetimes with a repulsive cosmological constant. The configurations are specified in terms of three parameters—the polytropic index n, the ratio of central pressure and central energy density of matter σ, and the ratio of energy density of vacuum and central density of matter λ. The static equilibrium configurations are determined by two coupled first-order nonlinear differential equations that are solved by numerical methods with the exception of polytropes with $n = 0$ corresponding to the configurations with a uniform distribution of energy density, when the solution is given in terms of elementary functions. The geometry of the polytropes is conveniently represented by embedding diagrams of both the ordinary space geometry and the optical reference geometry reflecting some dynamical properties of the geodesic motion. The polytropes are represented by radial profiles of energy density, pressure, mass, and metric coefficients. For all tested values of $n > 0$, the static equilibrium configurations with fixed parameters n, σ, are allowed only up to a critical value of the cosmological parameter $\lambda_c = \lambda_c(n, \sigma)$. In the case of $n > 3$, the critical value λ_c tends to zero for special values of σ. The gravitational potential energy and the binding energy of the polytropes are determined and studied by numerical methods. We discuss in detail the polytropes with an extension comparable to those of the dark matter halos related to galaxies, i.e., with extension $\ell > 100$ kpc and mass $M > 10^{12}\,M_\odot$. For such largely extended polytropes, the cosmological parameter relating the vacuum energy to the central density has to be larger than $\lambda = \rho_{vac}/\rho_c \sim 10^{-9}$. We demonstrate that the extension of the static general relativistic polytropic configurations cannot exceed the so-called static radius related to their external spacetime, supporting the idea that the static radius represents a natural limit on the extension of gravitationally bound configurations in an expanding universe dominated by the vacuum energy.

DOI: 10.1103/PhysRevD.94.103513

I. INTRODUCTION

Data from cosmological observations indicate that in the framework of the inflationary paradigm [1] a very small relict repulsive cosmological constant $\Lambda > 0$, i.e., vacuum energy or, generally, a dark energy demonstrating a repulsive gravitational effect, has to be invoked in order to explain the dynamics of the recent Universe [2–8]. The total energy density of the Universe is very close to the critical energy density ρ_{crit} corresponding to an almost flat universe predicted by the inflationary scenario [9]. Observations of distant Ia-type supernova explosions indicate that starting at the cosmological redshift $z \approx 1$ expansion of the Universe is accelerated [10]. The cosmological tests demonstrate convincingly that the dark energy represents about 70% of the energy content of the observable Universe [9,11]. These results are confirmed by recent measurements of cosmic microwave background anisotropies obtained by the space satellite observatory PLANCK [12,13].

There are strong indications that the dark energy equation of state is very close to those corresponding to the vacuum energy, i.e., to the repulsive cosmological constant [11]. Therefore, it is important to study the cosmological and astrophysical consequences of the effect of the observed cosmological constant implied by the cosmological tests to be $\Lambda \approx 1.3 \times 10^{-56}\ \mathrm{cm}^{-2}$ and the related vacuum energy $\rho_{vac} \sim 10^{-29}\ \mathrm{g/cm}^3$ that is comparable to the critical density of the Universe. The presence of a repulsive cosmological constant dramatically changes the asymptotic structure of black hole, naked singularity, or any compact-body backgrounds as such backgrounds become asymptotically de Sitter spacetimes, not flat spacetimes. In such spacetimes, an event horizon (cosmological horizon) always exists, behind which the geometry is dynamic.

The repulsive cosmological constant was discussed mainly in the scope of the cosmological models [14].

[*]Also at Research Centre of Theoretical Physics and Astrophysics, Faculty of Philosophy and Science, Silesian University in Opava, Bezručovo nám. 13, CZ-746 01 Opava, Czech Republic.
zdenek.stuchlik@fpf.slu.cz.
[†]Also at Research Centre of Computational Physica and Data Processing, Faculty of Philosophy and Science, Silesian University in Opava, Bezručovo nám. 13, CZ-746 01 Opava, Czech Republic.
stanislav.hledik@fpf.slu.cz.
[‡]jan.novotny@fpf.slu.cz

Its role in the vacuola models of mass concentrations immersed in the expanding universe has been considered in Refs. [15–20]. Recently, relevance of the repulsive cosmological constant has been found in the McVittie model [21] of mass concentrations immersed in the expanding universe [22–28]. A significant role of the repulsive cosmological constant has been demonstrated also for astrophysical situations related to active galactic nuclei and their central supermassive black holes [29]. The black-hole spacetimes with the Λ term are described in the spherically symmetric case by the vacuum Schwarzschild–(anti-)de Sitter (SdS) geometry [30,31], while the internal, uniform density SdS spacetimes are given in Refs. [32,33]. In the axially symmetric, rotating case, the vacuum spacetime is determined by the Kerr-de Sitter (KdS) geometry [34]. In the spacetimes with the repulsive cosmological term [and the related solutions of the f(R) gravity], motion of photons is treated in a series of papers [35–40,40–45], while motion of test particles was studied in Refs. [15,31, 46–68]. Oscillatory motion of current carrying string loops in SdS and KdS spacetimes was treated in Refs. [69–75].

The cosmological constant can be relevant in both the geometrically thin Keplerian accretion disks [29,31,47, 76,77] and the geometrically thick toroidal accretion disks 85–76]] orbiting supermassive black holes in the central parts of giant galaxies or in the recently discussed ringed accretion disks [86,87]. Spherically symmetric, stationary polytropic accretion in the spacetimes with the repulsive cosmological constant has been studied in Refs. [88–92].

In spherically symmetric spacetimes, Keplerian and toroidal disk structures can be described with high precision by an appropriately chosen pseudo-Newtonian potential [93,94] that appears to be useful also in studies of motion of interacting galaxies [95–97]. It should be mentioned that the KdS geometry can be relevant also in the case of Kerr superspinars representing an alternate explanation of active galactic nuclei [98–101]. The superspinars breaking the black-hole bound on the spin exhibit a variety of unusual physical phenomena [102–110].

Besides the vacuum black-hole (naked-singularity) spacetimes, we have to study the role of a repulsive cosmological constant also in nonvacuum spacetimes representing static mass configurations. Such general relativistic nonvacuum solutions can be interesting, e.g., in connection to the cold dark matter (CDM) halos that have been recently widely discussed as an explanation of the hidden structure of galaxies enabling the correct treatment of the motion in the external parts of galaxies [111,112] and are at present assumed usually in the Newtonian approximation [95,113–116]. There is a variety of candidates for the CDM [117]; nevertheless, none of these candidates is considered to be confirmed in the present state of knowledge. Therefore, it is important to test the possibility to represent such CDM halos in a relatively simple manner that enables us to estimate easily the role of the cosmological constant. We shall discuss the most simple case of spherically symmetric static configurations of perfect fluid with a polytropic equation of state generalizing thus the standard discussion of Tooper [118] by introducing the vacuum energy represented by the repulsive cosmological constant. Outside of these polytropic spheres, the spacetime is described by the vacuum SdS geometry.

Choosing the polytropic equation of state means that details of the processes inside the polytropic spheres are not considered, and a simple power law relating the total pressure to the total energy density of matter is assumed. Such an approximation seems to be applicable in the dark matter models that assume weakly interacting particles (see, e.g., Refs. [116,119,120]). In fact, such a simple assumption enables us to obtain basic properties of the nonvacuum configurations governed by the relativistic laws. For example, the equation of state of the ultrarelativistic degenerate Fermi gas is determined by the polytropic equation with the adiabatic index $\Gamma = 4/3$ corresponding to the polytropic index $n = 3$, while the nonrelativistic degenerate Fermi gas is determined by the polytropic equation of state with $\Gamma = 5/3$, and $n = 3/2$ [121]. It should be noted that a similar case of the adiabatic equation of state can be used in the case of a general ideal gas. This case was appropriately applied to describe the (test) perfect fluid toroidal configurations orbiting black holes [94] and can be, in principle, applied for the modeling of self-gravitating adiabatic spherically symmetric general relativistic configurations. The special case of polytropes with polytropic index $n = 0$ corresponding to the simplest, although rather unphysical and artificial, case of spheres with uniform distribution of energy density (but radius-dependent distribution of pressure) can be treated as a very useful model—it can serve as a test bed for properties of general relativistic polytropes (GRPs) because its structure equations can be solved in terms of elementary functions [32,33,122–124]. For nonzero values of the polytropic index, the structure equations have to be solved by numerical methods.

The Einstein equations with a nonzero cosmological constant lead in the case of spherically symmetric, static equilibrium configurations to generalized Tolman-Oppenheimer-Volkoff (TOV) equation. By using the standard ansatz for the polytropic equation of state, the equations are transferred into dimensionless form of two coupled first-order nonlinear differential equations that are solved by numerical methods under boundary conditions requiring regularity of the solution at the center of the polytrope and smooth matching of the internal spacetime at the surface of the polytrope to the external SdS spacetime characterized by the same mass parameter (and the cosmological constant) as the internal spacetime. The configurations are specified in terms of three parameters: the polytropic index n, the ratio of central pressure and central

energy density of matter σ, and the ratio of energy density of vacuum and central density of matter λ. By simultaneously solving the coupled equations, the structure of the polytrope is obtained; it is characterized by the profiles of the energy density, pressure, mass, and two metric coefficients (g_{tt}, g_{rr}) giving the geometry of the internal spacetime of the polytropic sphere. The spacetime structure can be reflected by the embedding diagrams of the ordinary space and the optical reference geometry reflecting some hidden properties of the spacetime [125,126]. The other relevant characteristics of the polytropes are the gravitational potential energy and the binding energy [118].

II. EQUATIONS OF STRUCTURE

In terms of the standard Schwarzschild coordinates, the line element of a spherically symmetric, static spacetime is given in the form

$$ds^2 = -e^{2\Phi}c^2dt^2 + e^{2\Psi}dr^2 + r^2(d\theta^2 + \sin^2\theta d\phi^2) \quad (1)$$

with just two unknown functions of the radial coordinate, $\Phi(r)$ and $\Psi(r)$. Matter inside the configuration is assumed to be a perfect fluid with $\rho = \rho(r)$ being the density of mass energy in the rest frame of the fluid and $p = p(r)$ being the isotropic pressure. The stress-energy tensor of the perfect fluid reads

$$T^{\mu}{}_{\nu} = (p + \rho c^2)U^{\mu}U_{\nu} + p\delta^{\mu}_{\nu}, \quad (2)$$

where U^{μ} denotes the 4-velocity of the fluid. We consider here the simplest direct relation between the energy density and pressure of the fluid given by the polytropic equation of state

$$p = K\rho^{1+\frac{1}{n}}, \quad (3)$$

where n is the "polytropic index" assumed to be a given constant (not necessarily an integer) and K is a constant that has to be determined by the thermal characteristics of a given fluid sphere, by specifying the density ρ_c and pressure p_c at the center of the polytrope. Since the density is a function of temperature for a given pressure, K contains the temperature implicitly. It can be shown that K is determined by the total mass, radius, and $p_c/\rho_c c^2$ ratio. (The polytropic equation represents a limiting form of the parametric equations of state for a completely degenerate gas at zero temperature, relevant, e.g., for neutron stars. Then, both n and K are universal physical constants [118].)

In a static configuration, each element of the fluid must remain at rest in the static coordinate system where the spatial components of 4-velocity field $dr/d\tau$, $d\theta/d\tau$, $d\phi/d\tau$ vanish, leaving the temporal component

$$u^t = \frac{dt}{d\tau} = e^{-\Phi} \quad (4)$$

as the only nonvanishing one. The structure of a relativistic star is determined by the Einstein field equations

$$G_{\mu\nu} \equiv R_{\mu\nu} - \frac{1}{2}Rg_{\mu\nu} + \Lambda g_{\mu\nu} = \frac{8\pi G}{c^4}T_{\mu\nu} \quad (5)$$

and by the law of local energy-momentum conservation

$$T^{\mu\nu}{}_{;\nu} = 0. \quad (6)$$

It is convenient to express the equations in terms of the orthonormal tetrad components using the 4-vectors carried by the fluid elements:

$$\vec{e}_{(t)} = \frac{1}{e^{\Phi}}\frac{\partial}{\partial t}, \qquad \vec{e}_{(r)} = \frac{1}{e^{\Psi}}\frac{\partial}{\partial r},$$
$$\vec{e}_{(\theta)} = \frac{1}{r}\frac{\partial}{\partial \theta}, \qquad \vec{e}_{(\phi)} = \frac{1}{r\sin\theta}\frac{\partial}{\partial \phi}. \quad (7)$$

Projection of $T^{\mu\nu}{}_{;\nu} = 0$ orthogonal to u^{μ} (by the projection tensor $P^{\mu\nu} = g^{\mu\nu} + u^{\mu}u^{\nu}$) gives the relevant equation

$$(\rho c^2 + p)\frac{d\Phi}{dr} = -\frac{dp}{dr}, \quad (8)$$

which is the equation of hydrostatic equilibrium describing the balance between the gravitational force and pressure gradient.

There are two relevant structure equations following from the Einstein equations. These are determined by the $(t)(t)$ and $(r)(r)$ tetrad components of the field equations [the $(\theta)(\theta)$ and $(\phi)(\phi)$ components give dependent equations]. First, we shall discuss the $(t)(t)$ component:

$$G_{(t)(t)} = \frac{1}{r^2} - \frac{e^{-2\Psi}}{r^2} - \frac{1}{r}\frac{d}{dr}e^{-2\Psi} - \Lambda = \frac{8\pi G}{c^2}\rho. \quad (9)$$

This can be transferred into the form

$$\frac{d}{dr}\left[r(1 - e^{-2\Psi}) - \frac{1}{3}\Lambda r^3\right] = \frac{d}{dr}\frac{2G}{c^2}m(r), \quad (10)$$

where

$$m(r) = \int_0^r 4\pi r'^2\rho dr'. \quad (11)$$

The integration constant in (11) is chosen to be $m(0) = 0$ because then the spacetime geometry is smooth at the origin (see Ref. [14]), and we arrive at the relation

$$e^{2\Psi} = \left[1 - \frac{2Gm(r)}{c^2 r} - \frac{1}{3}\Lambda r^2\right]^{-1}. \quad (12)$$

The $(r)(r)$ component of the field equations reads

$$G_{(r)(r)} = -\frac{1}{r^2} + \frac{e^{-2\Psi}}{r^2} + \frac{2e^{-2\Psi}}{r}\frac{d\Phi}{dr} + \Lambda = \frac{8\pi G}{c^4} p. \quad (13)$$

Using Eq. (12), we obtain the relation

$$\frac{d\Phi}{dr} = \frac{\frac{G}{c^2} m(r) - \frac{1}{3}\Lambda r^3 + \frac{4\pi G}{c^4} p r^3}{r[r - \frac{2G}{c^2} m(r) - \frac{1}{3}\Lambda r^3]}, \quad (14)$$

which enables us to put the equation of hydrostatic equilibrium (8) into the TOV form modified by the presence of a nonzero cosmological constant [32]:

$$\frac{dp}{dr} = -(\rho c^2 + p)\frac{\frac{G}{c^2} m(r) - \frac{1}{3}\Lambda r^3 + \frac{4\pi G}{c^4} p r^3}{r[r - \frac{2G}{c^2} m(r) - \frac{1}{3}\Lambda r^3]}. \quad (15)$$

The $(t)(t)$ component of the Einstein equations can be expressed and applied in the form

$$\frac{dm(r)}{dr} = 4\pi\rho(r) r^2. \quad (16)$$

For integration of the structure equations, it is convenient to introduce, following the approach of Ref. [118], a new variable θ related to the density radial profile $\rho(r)$ and the central density ρ_c, by

$$\rho = \rho_c \theta^n \quad (17)$$

with n being the polytropic index. The boundary condition on $\theta(r)$ reads $\theta(r=0) = 1$. The pressure dependence is given by the relation

$$p = K {\rho_c}^{1+\frac{1}{n}} \theta^{n+1}. \quad (18)$$

The conservation law (16) can be expressed in the form

$$\sigma(n+1) d\theta + (\sigma\theta + 1) d\Phi = 0, \quad (19)$$

where the parameter σ is given by the relation

$$\sigma = \frac{K}{c^2} {\rho_c}^{1/n} = \frac{p_c}{\rho_c c^2}. \quad (20)$$

At the edge of the configuration, $r = R$, there is $\rho(R) = p(R) = 0$. Outside the mass configuration with mass parameter M related to the mass of the polytrope by $M = m(R)$, the spacetime is described by the vacuum Schwarzschild–(anti-)de Sitter metric. Solving Eq. (19) and using the boundary condition that the internal and external metric coefficients are smoothly matched at $r = R$, we obtain

$$e^{2\Phi} = (1 + \sigma\theta)^{-2(n+1)} \left(1 - \frac{2GM}{c^2 R} - \frac{1}{3}\Lambda R^2\right). \quad (21)$$

Thus, the internal metric coefficient g_{tt} is determined by the function $\theta(r)$ and the parameter σ. The function $e^{2\Psi}$ remains to be expressed in terms of θ, and we need to find the function $\theta = \theta(r)$ using the structure equations. First, we rewrite Eq. (19) in the form

$$\frac{d\Phi}{dr} = \frac{\sigma(n+1)}{1 + \sigma\theta}\frac{d\theta}{dr}. \quad (22)$$

Then, we can express the $(r)(r)$ component of the Einstein equations and Eq. (16) in the form

$$\frac{\sigma(n+1)}{1+\sigma\theta} r \frac{d\theta}{dr}\left(1 - \frac{2Gm(r)}{c^2 r} - \frac{1}{3}\Lambda r^2\right) + \frac{Gm(r)}{c^2 r} - \frac{1}{3}\Lambda r^2 = -\frac{G}{c^2}\sigma\theta\frac{dm}{dr}, \quad (23a)$$

$$\frac{dm}{dr} = 4\pi r^2 \rho_c \theta^n. \quad (23b)$$

Introducing factor $\mathcal{L}$ giving a characteristic length scale of the polytrope

$$\mathcal{L} = \left[\frac{(n+1)K{\rho_c}^{1/n}}{4\pi G\rho_c}\right]^{1/2} = \left[\frac{\sigma(n+1)c^2}{4\pi G\rho_c}\right]^{1/2} \quad (24)$$

and factor $\mathcal{M}$ giving a characteristic mass scale of the polytrope

$$\mathcal{M} = 4\pi\mathcal{L}^3\rho_c = \frac{c^2}{G}\sigma(n+1)\mathcal{L}, \quad (25)$$

Eq. (23) can be transformed into dimensionless form by introducing a dimensionless radial coordinate

$$\xi = \frac{r}{\mathcal{L}} \quad (26)$$

and dimensionless quantities

$$v(\xi) = \frac{m(r)}{4\pi\mathcal{L}^3\rho_c} = \frac{m(r)}{\mathcal{M}}, \quad (27a)$$

$$\lambda = \frac{\rho_{vac}}{\rho_c}, \quad (27b)$$

where $v(\xi)$ represents a dimensionless mass parameter and λ represents a dimensionless cosmological constant related to the polytrope. The vacuum energy density is related to the cosmological constant by

$$\rho_{vac} c^2 = \frac{\Lambda c^4}{8\pi G} = \frac{8\pi G}{c^2}\rho_c\lambda. \quad (28)$$

The dimensionless form of Eq. (23) determining the polytrope structure then can be written down as

$$\frac{\mathrm{d}\theta}{\mathrm{d}\xi} = \frac{\frac{2}{3}\lambda\xi^3 - \sigma\xi^3\theta^{n+1} - v}{\xi^2(1+\sigma\theta)^{-1}}\, g_{rr}(\xi, v; n, \sigma, \lambda), \quad (29a)$$

$$\frac{\mathrm{d}v}{\mathrm{d}\xi} = \xi^2\theta^n, \quad (29b)$$

where

$$g_{rr}(\xi, v; n, \sigma, \lambda) \equiv \frac{1}{1 - 2\sigma(n+1)(\frac{v}{\xi} + \frac{1}{3}\lambda\xi^2)} \quad (30)$$

coincides with the radial metric coefficient (12). For given n, σ, and λ, Eq. (29) have to be simultaneously solved under the boundary conditions

$$\theta(0) = 1, \qquad v(0) = 0. \quad (31)$$

It follows from Eqs. (29b) and (31) that $v(\xi) \sim \xi^3$ for $\xi \to 0$ and, according to Eq. (29a),

$$\lim_{\xi\to 0_+} \frac{\mathrm{d}\theta}{\mathrm{d}\xi} = 0. \quad (32)$$

The boundary of the fluid sphere ($r = R$) is represented by the first zero point of $\theta(\xi)$, say at ξ_1:

$$\theta(\xi_1) = 0. \quad (33)$$

The solution ξ_1 determines the surface radius of the polytrope, and the solution $v(\xi_1)$ determines its gravitational mass.

In the Newtonian limit ($\sigma \ll 1$), the structure equations can be transformed to one differential equation of the second order,

$$\frac{1}{\xi^2}\frac{\mathrm{d}}{\mathrm{d}\xi}\left(\xi^2\frac{\mathrm{d}\theta}{\mathrm{d}\xi}\right) + \theta^n - 2\lambda = 0, \quad (34)$$

that is reduced to the Lane-Emden equation, if the cosmological term vanishes ($\lambda = 0$),

$$\frac{\mathrm{d}}{\mathrm{d}\xi}\left(\xi^2\frac{\mathrm{d}\theta}{\mathrm{d}\xi}\right) + \xi^2\theta^n = 0. \quad (35)$$

The differential equations governing the structure of GRPs have to be solved by numerical methods (even in the Newtonian limit). Only polytropes with the polytropic index $n = 0$, corresponding to configurations having uniform distribution of the energy density but nonuniform pressure profile, allow for solutions of the differential equations in terms of elementary functions.

III. PROPERTIES OF THE POLYTROPES

The general relativistic polytropic spheres with given polytropic index n are determined by the functions $\theta(\xi)$ and $v(\xi)$ of the dimensionless coordinate ξ and by the length and mass scales, $\mathcal{L}$ (24) and $\mathcal{M}$ (25). The functions $\theta(\xi)$ and $v(\xi)$ are governed by the structure equations, the values of the central energy density ρ_c, and the parameters σ and λ. A concrete polytropic sphere is then given by the first (lowest) solution ξ_1 of the equation $\theta(\xi) = 0$ that determines all the characteristics of the polytropic configuration and the radial profiles of its energy density, pressure, metric coefficients, or gravitational and binding energy.

Assuming Λ, n, σ, and ρ_c are given, then mass M, radius R, and the internal structure of the polytropes can be easily determined. First, the length scale $\mathcal{L}$ given by Eq. (24) has to be found. By numerical integration of Eq. (29), functions $\theta(\xi)$ and $v(\xi)$ are found, and ξ_1, where $\theta(\xi_1) = 0$, is determined together with $v(\xi_1)$. The radius of the sphere is

$$R = \mathcal{L}\xi_1, \quad (36)$$

and the mass of the sphere is given by

$$M = \mathcal{M}v(\xi_1) = \frac{c^2}{G}\mathcal{L}\sigma(n+1)v(\xi_1). \quad (37)$$

The density, pressure, and mass-distribution profiles are determined by the relations

$$\rho(\xi) = \rho_c\theta^n(\xi), \quad (38a)$$

$$p(\xi) = \sigma\rho_c\theta^{n+1}(\xi), \quad (38b)$$

$$M(\xi) = M\frac{v(\xi)}{v(\xi_1)}. \quad (38c)$$

The temporal and radial metric coefficients can be expressed in the form

$$\mathrm{e}^{2\Phi} = \frac{1 - 2\sigma(n+1)\left[\frac{v(\xi_1)}{\xi_1} + \frac{\lambda\xi_1^2}{3}\right]}{(1+\sigma\theta)^{2(n+1)}}, \quad (39a)$$

$$\mathrm{e}^{-2\Psi} = 1 - 2\sigma(n+1)\left[\frac{v(\xi)}{\xi} + \frac{1}{3}\lambda\xi^2\right] \quad (39b)$$

[see also Eq. (30)].

One of the basic characteristics of the polytropes is the mass-radius (M-R) relation. Using Eq. (27), we obtain

$$v(\xi) = \frac{m(r)}{4\pi\rho_c\mathcal{L}^2}\frac{\xi}{r} = \frac{G}{c^2\sigma(n+1)}\xi\frac{m(r)}{r}, \quad (40)$$

and the M-R relation can be expressed by the formula

$$\mathcal{C} \equiv \frac{GM}{c^2R} = \frac{1}{2}\frac{r_g}{R} = \frac{\sigma(n+1)v(\xi_1)}{\xi_1}, \quad (41)$$

where

$$r_g = \frac{2GM}{c^2} \tag{42}$$

is the gravitational radius of the polytropic configuration determined by its total gravitational mass M. The quantity $\mathcal{C}$ determines the compactness of the sphere, i.e., effectiveness of the gravitational binding, and it can be represented by the gravitational redshift of radiation emitted from the surface of the polytropic sphere [127].

The external vacuum SdS spacetime, with the same mass parameter M and the cosmological constant Λ as those characterizing the internal spacetime of the polytrope, has the metric coefficients

$$e^{2\Phi} = e^{-2\Psi} = 1 - \frac{2GM}{c^2 r} - \frac{1}{3}\Lambda r^2. \tag{43}$$

There are two pseudosingularities of the external vacuum geometry that give two length scales related to the polytropic spheres. The first one is determined by the radius of the black-hole horizon

$$r_h = \frac{2}{\sqrt{\Lambda}} \cos\frac{\pi + \alpha}{3}, \tag{44}$$

and the second one is given by the cosmological horizon

$$r_c = \frac{2}{\sqrt{\Lambda}} \cos\frac{\pi - \alpha}{3}; \tag{45}$$

there is

$$\alpha = \arccos\left(\frac{3}{2}\sqrt{\Lambda r_g^2}\right). \tag{46}$$

In astrophysically realistic situations, even for the most massive black holes in the central part of giant galaxies, such as the one observed in the quasar TON 618 with the mass $M \sim 6.6 \times 10^{10}\,M_\odot$ [128], or for whole giant galaxies containing an extended CDM halo and having mass up to $M \sim 10^{14}\,M_\odot$, the black-hole horizon and the cosmological horizon radii are given with very high precision by the simplified formulas

$$r_h = r_g, \qquad r_c = \left(\frac{1}{3}\Lambda\right)^{1/2}. \tag{47}$$

The horizons (black hole and cosmological) thus give two characteristic length scales of the SdS spacetimes. Clearly, the radius corresponding to the black hole horizon is located inside the polytropic spheres, while the cosmological horizon is located outside the polytropic sphere, usually at an extremely large distance from the polytrope for the observationally given value of the relict cosmological constant.

The Schwarzschild-de Sitter geometry can be characterized by a dimensionless parameter [31],

$$y = \frac{1}{12}\Lambda r_g^2. \tag{48}$$

Considering the observationally given repulsive cosmological constant $\Lambda = 1.3 \times 10^{-56}\ \mathrm{cm}^{-2}$, the cosmological parameter y takes extremely small values for astrophysically relevant objects such as the stellar mass black holes and galactic center black holes and even for the largest compact objects of the Universe, i.e., the central supermassive black holes in the active galactic nuclei or for the related giant galaxies [29,78]. However, we can introduce a third characteristic length scale determining the boundary of the gravitationally bound system, where cosmic repulsive effects start to be decisive. This is the so-called static radius [31,47,95,97,129,130] defined as

$$r_s = \frac{r_g}{2y^{1/3}}. \tag{49}$$

At the static radius, the gravitational attraction of the central mass source is just balanced by the cosmic repulsion, and behind the static radius, the cosmic repulsive acceleration prevails [29].

It is relevant and instructive to relate the three characteristic length scales of the external vacuum spacetime to the length scale of the general relativistic polytrope $\mathcal{L}$ and its radius $R = \mathcal{L}\xi_1$. In the case of polytropes with very large central density, related to the central densities of neutron stars, quark stars, or other very compact objects, the polytrope length scale is comparable to the scale of the black-hole horizon, while with decreasing central density the polytrope length scale increases in comparison to the black-hole horizon scale. In the case of extremely low central densities related to extremely extended polytropes that could represent, e.g., the CDM halos, their length scale is comparable to the static radius of the external spacetime. We shall see that the static radius cannot be exceeded by the polytrope extension. For observationally given cosmological constant, the length scale (extension) of all astrophysically relevant polytropes is much lower than the length scale of the cosmological horizon.

IV. GRAVITATIONAL ENERGY AND BINDING ENERGY OF THE POLYTROPIC SPHERES

Properties of the GRPs are well characterized by their gravitational potential energy and binding energy. The latter reflects amount of the microscopic kinetic energy bounded in the relativistic polytropes. Both the (negative) gravitational potential energy and the binding energy are related to the total energy given by the mass parameter of the polytropes and are expressed in terms of the parameters characterizing the polytropes that can be determined

numerically. In the case of the $n = 0$ polytropes, the binding energy must be just negatively valued gravitational potential energy, because the polytropic configurations with uniform distribution of energy density have to be considered as incompressible.

A. Gravitational potential energy

Because of the equivalence of matter and energy, the total energy E of the mass configuration, including the internal energy and gravitational potential energy, is given by the gravitational mass M generating the external gravitational field:

$$E = Mc^2 = 4\pi c^2 \mathcal{L}^3 \rho_c v(\xi_1) = 4\pi c^2 \int_0^R \rho r^2 \mathrm{d}r. \quad (50)$$

The proper energy E_0 is defined as the integral of the energy density over the proper volume of the fluid sphere

$$E_0 = 4\pi c^2 \mathcal{L}^3 \rho_c \int_0^{\xi_1} g_{rr}^{1/2} \theta^n \xi^2 \mathrm{d}\xi \quad (51)$$

with $g_{rr}(\xi, v; n, \sigma, \lambda)$ given by Eq. (30). The gravitational potential energy is thus given by

$$\mathcal{G} = E - E_0. \quad (52)$$

Since $\mathrm{e}^{\Psi} \geq 1$, there is $E_0 \geq E$ and $\mathcal{G} \leq 0$—the gravitational potential energy is always negative. Following the basic work of Tooper [118], we can consider the negatively valued gravitational potential energy, $(-\mathcal{G})$, as the gravitational binding energy, i.e., the energy representing the work that has to be applied to the system in order to disperse the matter against the gravitational forces. The intensity of the gravitational binding of the polytropic spheres can be represented by the ratio

$$g = \frac{\mathcal{G}}{E} = 1 - \frac{1}{v(\xi_1)} \int_0^{\xi_1} g_{rr}^{1/2} \theta^n \xi^2 \mathrm{d}\xi. \quad (53)$$

The proper energy of a relativistic polytrope consists of the rest energy of gas, the kinetic energy of microscopic motion of the gas, and the radiation energy. The simple polytropic law relates the total energy density and the total pressure, which consists of gas pressure related to the kinetic energy of the microscopic motion, and the radiation pressure. Therefore, we have to determine the gas density of the polytropic matter.

B. Adiabatic processes and speed of sound

In the relativistic polytropes, the special case of adiabatic processes implies a unique relation between the gas density ρ_g and the total mass density ρ, or between ρ_g and θ [118]. The assumption of an adiabatic process is consistent with the absence of heat terms in the energy-momentum tensor. For an adiabatic process, the relativistic generalization of the first law of thermodynamics takes the form

$$\mathrm{d}\epsilon + (p + \epsilon)\frac{\mathrm{d}V}{V} = 0, \quad (54)$$

where $\mathrm{d}\epsilon$ is the change in the energy density due to a change $\mathrm{d}V$ in the specific volume. Since

$$\frac{\mathrm{d}V}{V} = -\frac{\mathrm{d}\rho_g}{\rho_g}, \quad (55)$$

we arrive at

$$\frac{\mathrm{d}\rho_g}{\rho_g} = \frac{\mathrm{d}\epsilon}{p + \epsilon}, \quad (56)$$

and using the variable θ, we find the equation

$$\frac{\mathrm{d}\rho_g}{\rho_g} = \frac{n\mathrm{d}\theta}{\theta(1 + \sigma\theta)}. \quad (57)$$

Because the internal energy density is small compared to the rest energy density near the boundary of the polytropic sphere, we obtain the profile of the rest mass density in the form

$$\rho_g = \rho_c \left(\frac{\theta}{1 + \sigma\theta}\right)^2 = \frac{\rho}{(1 + \sigma\theta)^n}. \quad (58)$$

In the nonrelativistic limit ($\sigma \ll 1$), the gas density and the total density are nearly equal.

The standard relativistic (Landau-Lifshitz) formula for the phase velocity of sound in an adiabatic process [131]

$$v_s^2 = \left(\frac{\mathrm{d}p}{\mathrm{d}\rho}\right)_{\text{adiabatic}} \quad (59)$$

yields the phase sound speed at the center of the polytrope to be given by

$$v_{sc} = c\left(\frac{n+1}{n}\sigma\right)^{1/2}. \quad (60)$$

For a given n, there is a maximum value of the parameter σ that guarantees $v_{sc} < c$:

$$\sigma \leq \frac{n}{n+1}. \quad (61)$$

For the nonrelativistic Fermi gas $n = 3/2$, we have $\sigma_N \leq 3/5$, while for the ultrarelativistic Fermi gas $n = 3$, we have $\sigma_U \leq 3/4$; for the case of $n = 4$, there is $\sigma \leq 4/5$. However, these limits hold for the phase sound velocity, not the group velocity, so they should not be taken too literally [118].

C. Binding energy

The proper mass and the total rest energy of gas in a polytropic sphere are determined by the relation

$$E_{0\mathrm{g}} = M_{0\mathrm{g}}c^2 = 4\pi c^2 \int_0^R \rho_{\mathrm{g}} \mathrm{e}^{\Psi} r^2 \mathrm{d}r. \tag{62}$$

The energy $E_{0\mathrm{g}}$ represents the sum of the rest masses of the elementary particles in the polytrope in units of energy, and $M_{0\mathrm{g}}$ gives the number of nucleons in the polytrope multiplied by the nucleon rest mass. The proper rest energy of the gas in the polytropic configuration is given by integration over the proper volume and is determined by the relation

$$E_{0\mathrm{g}} = 4\pi c^2 \mathcal{L}^3 \rho_{\mathrm{c}} \int_0^{\xi_1} \frac{g_{rr}^{1/2}\theta^n \xi^2 \mathrm{d}\xi}{(1+\sigma\theta)^n} \tag{63}$$

with $g_{rr}(\xi, v; n, \sigma, \lambda)$ given by Eq. (30). The binding energy E_{b} of the gas of the polytropic sphere is then given by the formula

$$E_{\mathrm{b}} = E_{0\mathrm{g}} - E. \tag{64}$$

Considering an "initial" state where the particles are widely dispersed and the system has zero internal energy, and assuming conservation of the number of nucleons, the binding energy represents the difference in energy between the initial state and the "final" state in which the particles with given internal energy are bounded by gravitational forces.

We can consider the quantity giving the difference of the proper energy E_0 and the proper rest energy $E_{0\mathrm{g}}$, describing the internal "kinetic" energy of the polytropic sphere (more precisely of particles constituting the polytrope):

$$E_{\mathrm{k}} = E_0 - E_{0\mathrm{g}}. \tag{65}$$

Polytropic fluid spheres can be characterized by relating the gravitational potential energy, the binding energy, and the kinetic energy to the total energy, introducing the following parameters: the internal energy parameter

$$i \equiv \frac{E_{0\mathrm{g}}}{E} = \frac{1}{v(\xi_1)} \int_0^{\xi_1} \frac{g_{rr}^{1/2}\theta^n \xi^2 \mathrm{d}\xi}{(1+\sigma\theta)^n}; \tag{66}$$

binding energy parameter

$$b \equiv \frac{E_{\mathrm{b}}}{E} = \frac{E_{0\mathrm{g}}}{E} - 1 = i - 1; \tag{67}$$

and the kinetic energy parameter

$$k \equiv \frac{E_{\mathrm{k}}}{E} = \frac{E_0}{E} - \frac{E_{0\mathrm{g}}}{E}. \tag{68}$$

Clearly, the parameters are not independent. They are related by

$$k = 1 - g - i = -g - b. \tag{69}$$

It is not apparent if the binding energy is positive or negative. The gas density ρ_{g} is smaller than the total density ρ, but the radial metric coefficient is in general greater than unity. Recall that in the Newtonian limit (with $\lambda = 0$) we obtain in the first approximation

$$\begin{aligned} E_0 &\approx 4\pi c^2 \int_0^R \rho(r)\left[1 + \frac{Gm(r)}{c^2 r}\right] r^2 \mathrm{d}r \\ &= E + \int_0^R \frac{Gm(r)\mathrm{d}m(r)}{r} \end{aligned} \tag{70}$$

and the binding energy is determined by the well-known formula [121]

$$E_{\mathrm{b}} \approx \frac{3-n}{5-n}\frac{GM^2}{R} \approx \frac{n-3}{3}G. \tag{71}$$

The Newtonian limit demonstrates immediately that the binding energy can be positive or negative, in dependence on the polytropic index n. Since the gravitational energy is always negative, we can conclude that in this limit the binding energy is positive (negative) for $n < 3$ ($n > 3$). In the fully general relativistic polytropes, the situation is clearly more complex. The fully general relativistic polytropic spheres are characterized by the most important quantity relating the binding energy and the gravitational potential energy through the formula

$$\frac{E_{\mathrm{b}}}{G} = \frac{\int_0^{\xi_1} \frac{g_{rr}^{1/2}\theta^n \xi^2 \mathrm{d}\xi}{(1+\sigma\theta)^n} - v(\xi_1)}{v(\xi_1) - \int_0^{\xi_1} g_{rr}^{1/2}\theta^n \xi^2 \mathrm{d}\xi} \tag{72}$$

that enables us to find easily the regions of positively valued binding energy since the gravitational energy is again always negative.

V. EMBEDDINGS OF THE ORDINARY AND OPTICAL SPACE

We concentrate our attention on the visualization of the structure of the internal spacetime of the GRPs, considering both the ordinary and the optical geometry of the spacetime.

The curvature of the internal spacetime of the polytropes can conveniently be represented by the standard embedding of 2D, appropriately chosen, spacelike surfaces of the ordinary 3-space of the geometry (here, these are $t =$ const sections of the central planes) into 3D Euclidean space [14].

The 3D optical reference geometry [132], associated with the spacetime under consideration, enables the introduction of a natural "Newtonian" concept of gravitational and inertial forces and reflects some hidden properties of the test particle motion [125,126,133,134]. (In accord with the spirit of general relativity, alternative approaches to the concept of inertial forces are possible, e.g., the "special relativistic" one [135].) Properties of the inertial forces can be reflected by the embedding diagrams of appropriately chosen 2D sections of the optical geometry, as reviewed, e.g., in Refs. [126,136]. The embedding diagrams of the $n = 0$ polytropes with the uniform distribution of the energy density were presented in Ref. [122]; here, they are constructed for typical GRPs with $n > 0$. Note that it can be directly shown by using the optical reference geometry that extremely compact configurations, allowing the existence of bound null geodesics, can exist [122,137]. Such extremely compact relativistic polytropes have a turning point of the embedding diagram of the optical geometry as shown in Ref. [126]. However, as we show later, such configurations can have compactness parameter $\mathcal{C} > 1/3$.

We embed the equatorial plane of the ordinary space geometry and optical reference geometry into the 3D Euclidean space with the line element

$$\mathrm{d}\tilde{\sigma}^2 = \mathrm{d}\rho^2 + \rho^2\mathrm{d}\alpha^2 + \mathrm{d}z^2. \tag{73}$$

The embedding is a rotationally symmetric surface $z = z(\rho)$ with the line element (2D):

$$\mathrm{d}\ell^2_{(\mathrm{E})} = \left[1 + \left(\frac{\mathrm{d}z}{\mathrm{d}\rho}\right)^2\right]\mathrm{d}\rho^2 + \rho^2\mathrm{d}\alpha^2. \tag{74}$$

A. Ordinary space

Its equatorial plane has the line element

$$\mathrm{d}\ell^2_{(\mathrm{ord})} = g_{rr}\mathrm{d}r^2 + r^2\mathrm{d}\phi^2, \tag{75}$$

where

$$g_{rr} = \mathrm{e}^{2\Psi(r)} = \left\{1 - 2\sigma(n+1)\left[\frac{v(\xi)}{\xi} + \frac{\lambda}{3}\xi^2\right]\right\}^{-1} \tag{76}$$

with $v(\xi)$ being the solution of the TOV for the GRP. We have to identify $\mathrm{d}\ell^2_{(\mathrm{E})}$ and $\mathrm{d}\ell^2_{(\mathrm{ord})}$. Clearly, $\alpha \equiv \phi$, and $\rho \equiv r$. The embedding formula then takes the form

$$\frac{\mathrm{d}z}{\mathrm{d}r} = \pm\sqrt{g_{rr} - 1}; \tag{77}$$

different signs give isometric surfaces. We take + sign. Using Eq. (76), we arrive at the dimensionless embedding formula if we introduce

$$z = \frac{z}{\mathcal{L}}, \qquad \xi = \frac{r}{\mathcal{L}} \tag{78}$$

in the form

$$\frac{\mathrm{d}z}{\mathrm{d}\xi} = \left\{\frac{2\sigma(n+1)[\frac{v(\xi)}{\xi} + \frac{\lambda}{3}\xi^2]}{1 - 2\sigma(n+1)[\frac{v(\xi)}{\xi} + \frac{\lambda}{3}\xi^2]}\right\}^{1/2}. \tag{79}$$

This must be integrated numerically using a computer code for $v(\xi)$. Clearly, the embedding is well defined in the whole range of allowed $\xi \in (0, \xi_1)$, as $g_{rr} > 1$ there.

B. Optical space (optical reference geometry)

In the static spacetimes, the optical 3D space has its metric coefficients determined by [132,138]

$$h_{ik} = \frac{g_{ik}}{-g_{tt}}. \tag{80}$$

Its equatorial plane has the line element

$$\mathrm{d}\ell^2_{(\mathrm{opt})} = h_{rr}\mathrm{d}r^2 + h_{\phi\phi}\mathrm{d}\phi^2 \tag{81}$$

that has to be identified with $\mathrm{d}\ell^2_{(\mathrm{E})}$. Now, the azimuthal coordinates still can be identified ($\alpha \equiv \phi$); however, the radial coordinates are related via

$$\rho^2 = h_{\phi\phi}, \tag{82}$$

and the embedding formula is given by

$$\frac{\mathrm{d}z}{\mathrm{d}\rho} = h_{rr}\left(\frac{\mathrm{d}r}{\mathrm{d}\rho}\right)^2 - 1. \tag{83}$$

It is convenient to cast the embedding formula into a parametric form $z(\rho) = z(r(\rho))$. Then,

$$\frac{\mathrm{d}z}{\mathrm{d}r} = \sqrt{h_{rr} - \left(\frac{\mathrm{d}\rho}{\mathrm{d}r}\right)^2}. \tag{84}$$

Because

$$\frac{\mathrm{d}z}{\mathrm{d}\rho} = \frac{\mathrm{d}z}{\mathrm{d}r}\frac{\mathrm{d}r}{\mathrm{d}\rho}, \tag{85}$$

the turning points of the embedding diagrams are given by the condition

$$\frac{\mathrm{d}\rho}{\mathrm{d}r} = 0. \tag{86}$$

The reality condition, determining the limits of embeddability, reads

$$h_{rr} - \left(\frac{\mathrm{d}\rho}{\mathrm{d}r}\right)^2 \geq 0. \tag{87}$$

For the GRPs, the metric coefficients of the optical geometry are given by the formulas

$$h_{rr} = \frac{\mathrm{e}^{2\Psi}}{\mathrm{e}^{2\Phi}} = \frac{[1+\sigma\theta(\xi)]^{2(n+1)}}{1-2\sigma(n+1)[\frac{v(\xi_1)}{\xi_1}+\frac{\lambda}{3}\xi_1^2]} \times \left\{1-2\sigma(n+1)\left[\frac{v(\xi)}{\xi}+\frac{\lambda}{3}\xi^2\right]\right\}, \tag{88}$$

$$h_{\phi\phi} = \frac{r^2}{\mathrm{e}^{2\Phi}} = \frac{r^2[1+\sigma\theta(\xi)]^{2(n+1)}}{1-2\sigma(n+1)[\frac{v(\xi_1)}{\xi_1}+\frac{\lambda}{3}\xi_1^2]}. \tag{89}$$

Introducing a dimensionless coordinate η by

$$\eta = \frac{\rho}{\mathcal{L}}, \tag{90}$$

we can write

$$\eta = \frac{\xi[1+\sigma\theta(\xi)]^{n+1}}{\{1-2\sigma(n+1)[\frac{v(\xi_1)}{\xi_1}+\frac{\lambda}{3}\xi_1^2]\}^{1/2}} \tag{91}$$

and

$$\frac{\mathrm{d}\eta}{\mathrm{d}\xi} = \frac{\xi[1+\sigma\theta(\xi)]^n\{1+\sigma[\theta(\xi)+(n+1)\xi\frac{\mathrm{d}\theta}{\mathrm{d}\xi}]\}}{\{1-2\sigma(n+1)[\frac{v(\xi_1)}{\xi_1}+\frac{\lambda}{3}\xi_1^2]\}^{1/2}}. \tag{92}$$

The condition for the turning points of the embedding diagrams thus reads

$$\theta(\xi) + (n+1)\xi\frac{\mathrm{d}\theta}{\mathrm{d}\xi} = -\frac{1}{\sigma}. \tag{93}$$

The embedding formula takes the form

$$\left(\frac{\mathrm{d}z}{\mathrm{d}\xi}\right)^2 = \left\{1-2\sigma(n+1)\left[\frac{v(\xi_1)}{\xi_1}+\frac{\lambda}{3}\xi_1^2\right]\right\}\left\{1-2\sigma(n+1)\left[\frac{v(\xi)}{\xi}+\frac{\lambda}{3}\xi^2\right]\right\}2\sigma(n+1)[1+\sigma\theta(\xi)]^{2n} \times \left\{\left\{1+\sigma\left[\theta(\xi)+(n+1)\xi\frac{\mathrm{d}\theta}{\mathrm{d}\xi}\right]\right\}\left[\frac{v(\xi)}{\xi}+\frac{\lambda}{3}\xi^2\right]-\xi\frac{\mathrm{d}\theta}{\mathrm{d}\xi}\left[1+\sigma\theta(\xi)+\frac{\sigma}{2}(n+1)\xi\frac{\mathrm{d}\theta}{\mathrm{d}\xi}\right]\right\}. \tag{94}$$

This has to be solved numerically, together with the condition on the limits of embeddability given in the form

$$\left\{1+\sigma\left[\theta(\xi)+(n+1)\xi\frac{\mathrm{d}\theta}{\mathrm{d}\xi}\right]\right\}\left[\frac{v(\xi)}{\xi}+\frac{\lambda}{3}\xi^2\right] - \xi\frac{\mathrm{d}\theta}{\mathrm{d}\xi}\left[1+\sigma\theta(\xi)+\frac{\sigma}{2}(n+1)\xi\frac{\mathrm{d}\theta}{\mathrm{d}\xi}\right] \geq 0. \tag{95}$$

VI. CONFIGURATIONS OF UNIFORM DENSITY

There is a special class of GRPs of the index $n = 0$ where the structure equations can be integrated in terms of elementary functions. We shall discuss these polytropes in detail because they can give an intuitive insight into the role of the cosmological constant and can serve as a test bed for the general case of polytropes with $n > 0$.

The $n = 0$ polytropes correspond to the special class of the internal Schwarzschild–(anti-)de Sitter spacetimes [32] where the distribution of density ρ is uniform although the pressure grows monotonically from its zero value on the surface of the configuration to a maximum value at its center. Recall that in the configurations with $\rho = \text{const}$ it is not necessary to use the unrealistic notion of an incompressible fluid—one can consider fluids with pressure growing as radius decreases, being "hand tailored" [14]. Assuming $n = 0$, Eq. (29b) can be integrated to give

$$v(\xi) = \frac{1}{3}\xi^3, \tag{96}$$

while Eq. (29a) takes the form

$$[3-2\sigma(1+\lambda)\xi^2]\frac{\mathrm{d}\theta}{\mathrm{d}\xi} + (1-2\lambda+3\sigma\theta)(1+\sigma\theta) = 0 \tag{97}$$

and can be integrated directly after separation of variables. Using the boundary condition $\theta(0) = 1$, we obtain

$$\sigma\theta = \frac{1-\frac{(1-2\lambda)(1+\sigma)}{(1-2\lambda+3\sigma)[1-\frac{2}{3}\sigma(1+\lambda)\xi^2]^{1/2}}}{\frac{3(1+\sigma)}{(1-2\lambda+3\sigma)[1-\frac{2}{3}\sigma(1+\lambda)\xi^2]^{1/2}}-1}. \tag{98}$$

This solution determines the dependence of pressure on the radial coordinate, since for $n = 0$ there is $\theta = p(r)/p_c$. The dependence is given in units of the energy density since $\sigma = p_c/\rho_c$. From the condition $\theta(\xi_1) = 0$, we find the radius of the configuration to be determined by

$$\xi_1^2(\sigma,\lambda) = \frac{6[1+2\sigma-\lambda(2+\sigma)]}{(1-2\lambda+3\sigma)^2}. \tag{99}$$

We illustrate behavior of the function $\xi_1^2(\sigma,\lambda)$ in Fig. 1. Clearly, the parameters σ and λ have to be restricted by the condition

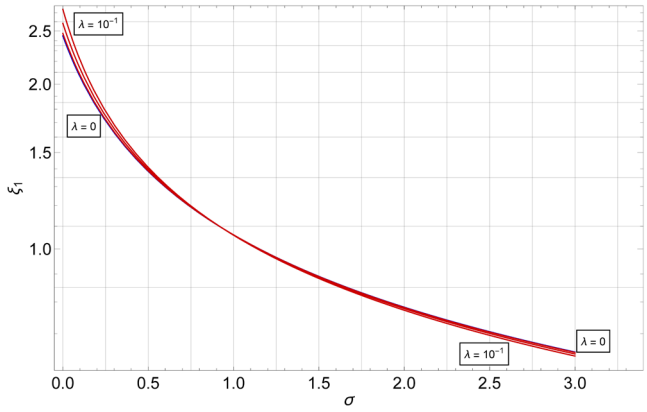

FIG. 1. Dependence of the dimensionless radius ξ_1 (99) for configurations of uniform density on relativity parameter σ for cosmological parameter $\lambda=0,10^{-2},5\times10^{-2},10^{-1}$, respectively.

$$\lambda \leq \frac{1+2\sigma}{2+\sigma}. \tag{100}$$

However, the $n=0$ polytropic configurations should behave regularly for all allowed values of the relativistic parameter $\sigma>0$, but $\xi_1^2(\sigma,\lambda)$ always diverges for σ low enough, if $\lambda>1/2$. Therefore, it is natural to put the restriction of

$$\lambda \leq \frac{1}{2}. \tag{101}$$

We can express the pressure profile in terms of r, R, instead of ξ, ξ_1 and σ, λ, obtaining thus the form of the expression of the $n=0$ polytrope as being discussed in Ref. [32]. Introducing a new parameter a, having dimension of length, by the relation

$$\frac{1}{a^2}=\frac{8\pi}{3}(\rho_c+\rho_{vac}), \tag{102}$$

we find the relation of R, σ, and λ to be given by

$$\left(1-\frac{R^2}{a^2}\right)^{1/2}=\frac{(1-2\lambda)(1+\sigma)}{1-2\lambda+3\sigma}. \tag{103}$$

The central pressure p_c and the pressure profile $p(r)$ can be then expressed in the known form [32,139]

$$p_c=\rho_c\frac{(1-2\lambda)[1-(1-\frac{R^2}{a^2})^{1/2}]}{3(1-\frac{R^2}{a^2})^{1/2}-(1-2\lambda)}, \tag{104a}$$

$$p(r)=\rho_c\frac{(1-2\lambda)[(1-\frac{r^2}{a^2})^{1/2}-(1-\frac{R^2}{a^2})^{1/2}]}{3(1-\frac{R^2}{a^2})^{1/2}-(1-2\lambda)(1-\frac{r^2}{a^2})^{1/2}}. \tag{104b}$$

The presented results for the $n=0$ polytropes are relevant for both the positive and negative values of the cosmological parameter λ describing thus also effects of the attractive cosmological constant when $\lambda<0$.

The radial metric coefficient is given by the relation

$$e^{2\Psi(r)}=\left(1-\frac{r^2}{a^2}\right)^{-1}, \tag{105}$$

and the total mass reads

$$M=\frac{1}{3}\mathcal{L}\sigma\xi_1^3=\frac{4\pi}{3}\rho_c r^3. \tag{106}$$

The temporal metric coefficient is determined by the relations

$$e^{\Phi(r)}=\frac{[1-\frac{2}{3}\sigma(1+\lambda)\xi^2]^{1/2}}{1+\sigma\theta}, \tag{107a}$$

$$e^{\Phi(r)}=\frac{3(1-\frac{R^2}{a^2})^{1/2}-(1-2\lambda)(1-\frac{r^2}{a^2})^{1/2}}{2(1+\lambda)}. \tag{107b}$$

The special case of the attractive cosmological constant corresponding to $\lambda=-1$ has to be treated separately as $1/a^2=0$. In such a case, Eq. (97) reduces to

$$\frac{d\theta}{(1+\sigma\theta)^2}=-\xi d\xi, \tag{108}$$

which leads, after integration with the boundary condition $\theta(0)=1$, to the formula

$$\theta=\frac{1-\frac{1}{2}(1+\sigma)\xi^2}{1+\frac{1}{2}(1+\sigma)\xi^2}. \tag{109}$$

The boundary of the configuration is at

$$\xi_1^2=\frac{2}{1+\sigma}. \tag{110}$$

The central pressure and the pressure profile can be expressed in terms of the radial coordinates r, R in the form

$$p_c=\frac{\rho_c}{(\frac{2R}{3M}-1)}, \tag{111a}$$

$$p(r)=p_c\frac{1-\frac{r^2}{R^2}}{1+\frac{1}{\frac{2R}{3M}-1}\frac{r^2}{R^2}}. \tag{111b}$$

The metric coefficients have a special form, too. The radial g_{rr} component corresponds to the flat $t=$ const sections

$$e^{2\Psi(r)}=1, \tag{112}$$

while the temporal g_{tt} component takes the form [32]

$$e^{\Phi(r)} = 1 + \frac{3M}{2R}\left(\frac{r^2}{R^2} - 1\right). \tag{113}$$

Properties of the $n = 0$ GRPs were discussed in Refs. [32,122]. In the following, we concentrate on the existence of these polytropes in dependence on the repulsive cosmological constant.

A. Existence conditions of the $n = 0$ polytropes and their compactness

The reality conditions on the general solution, given by Eqs. (104), (105), and (107b), must guarantee that the pressure is positive and nondivergent, and the metric coefficients have to be regular at $r \leq R$. Therefore, two conditions have to be satisfied:

$$1 - 2\lambda > 0 \tag{114}$$

and

$$3\left(1 - \frac{R^2}{a^2}\right)^{1/2} - (1 - 2\lambda) > 0. \tag{115}$$

Considering the limiting case of $\lambda = 1/2$, we find

$$\theta(\xi) = \frac{(1 - \sigma\xi^2)^{1/2}}{1 + \sigma + \sigma(1 - \sigma\xi)^{1/2}}. \tag{116}$$

The boundary of such a polytrope configuration is at

$$\xi_1^2 = \frac{1}{\sigma}, \tag{117}$$

and we can show that

$$R^2 = a^2. \tag{118}$$

Therefore, the metric coefficients are singular because there is

$$e^{-2\Psi(R)} = e^{2\Phi(R)} = e^{2\Phi(r)} = 1 - \frac{R^2}{a^2}. \tag{119}$$

For polytrope configurations of a given M and $\Lambda > 0$, condition (114) gives an upper limit on admissible values of the external radius R. Configurations with $\lambda \sim 1/2$ can be considered as nearly "geodetical" since the pressure gradient almost vanishes on the surface, which is close to the static radius of the external geometry. (For $\lambda = 1/2$, the surface of the static configuration has to be located at the horizon of the external spacetime, with $R = 3r_g/3$; however, no static configuration can have its boundary at a black-hole horizon, and such configurations are forbidden.)

The lower limit on the external radius of the $n = 0$ polytropes is determined by the condition (115) that can be transformed into the relations

$$\frac{R^2}{a^2} < \frac{4(1 + \lambda)(2 - \lambda)}{9} \tag{120}$$

and

$$R > 2M\frac{9}{4(2 - \lambda)}. \tag{121}$$

For $\lambda = 0$, we obtain the well-known limit $R > (9/4)(GM/c^2)$. The restrictions on physically realistic $n = 0$ polytropes can also be transformed into a form containing dimensionless quantities $x \equiv R/M$, $y \equiv \Lambda M^2/3$ (see Refs [32,122]).

Compactness of the polytropic spheres of the uniform density is given by the relation

$$\mathcal{C}(\sigma, \lambda) = \frac{2\sigma[1 - 2\lambda + \sigma(2 - \lambda)]}{(1 - 2\lambda + 3\sigma)^2} \tag{122}$$

that is reduced for $\lambda = 0$ to the formula

$$\mathcal{C}(\sigma) = \frac{2\sigma(1 + 2\sigma)}{(1 + 3\sigma)^2}. \tag{123}$$

The extremely compact configurations with $\mathcal{C} > 1/3$ can exist, if the central parameter satisfies the relation

$$\sigma^2 \geq \sigma_{\rm ext}^2 \equiv \frac{2}{3}\lambda. \tag{124}$$

Note that extremely compact spherical configurations have their surface located under the photon circular orbit of the external spacetime [140]. It can be shown [122] that in extremely compact configurations (with $R < 3M$) a stable circular null geodesic exists around which null geodesics captured by the strong gravitational field are concentrated. Neutrinos, moving along these bound null geodesics, can influence cooling of extremely compact neutron stars. The potential well of the captured geodesics becomes deeper with the repulsive cosmological constant increasing, while it gets flatter with the attractive cosmological constant decreasing [137].

B. Gravitational binding of the $n = 0$ polytropes

It is instructive to give the gravitational energy of the $n = 0$ polytropes and their gravitational binding factor g. The total energy takes the simple form

$$E = M = \frac{4\pi}{3}\rho_c R^3. \tag{125}$$

The formula for the total proper energy reads

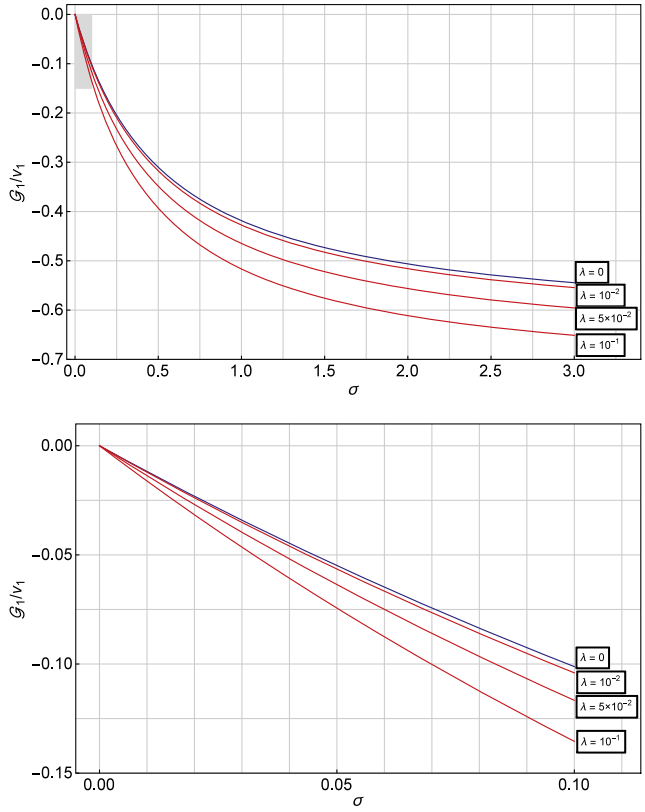

FIG. 2. Dependence of the gravitational binding factor (130) for configurations of uniform density on relativity parameter σ for cosmological parameter $\lambda = 0, 10^{-2}, 5\times10^{-2}, 10^{-1}$, respectively. The "1" index emphasizes the energies are related to the whole configuration. *Top:* Wide range of relativity parameter. *Bottom:* Zoom of the shaded region in the top plot.

$$E_0 = 4\pi\rho_c \int_0^R \left(1-\frac{r^2}{a^2}\right)^{-1/2} r^2 \mathrm{d}r; \tag{126}$$

after integration, we obtain

$$E_0 = \frac{3M}{2}\left(\frac{a}{R}\right)^3\left[\arcsin\left(\frac{R}{a}\right) - \frac{R}{a}\left(1-\frac{R^2}{a^2}\right)^{1/2}\right], \tag{127}$$

where

$$\frac{R}{a} = \frac{2(1+\lambda)^{1/2}}{1-2\lambda+3\sigma}\{\sigma[1+2\sigma-\lambda(2+\sigma)]\}^{1/2}. \tag{128}$$

The gravitational potential energy can be given in the form

$$\mathcal{G} = Mc^2 g, \tag{129}$$

where the negative gravitational binding factor $g = \mathcal{G}/E$ is given in terms of the R/a ratio,

$$g = 1 - \frac{3}{2}\left(\frac{a}{R}\right)^3\left[\arcsin\left(\frac{R}{a}\right) - \frac{R}{a}\left(1-\frac{R^2}{a^2}\right)^{1/2}\right]. \tag{130}$$

It expresses the gravitational binding in a "pure" form as there in no internal energy in "incompressible" configurations. We can directly conclude that the relation of the binding energy of gas E_b and the gravitational energy is given by

$$\frac{E_b}{\mathcal{G}} = -1. \tag{131}$$

The gravitational potential energy of the $n = 0$ GRP is represented in Fig. 2. The role of the cosmological constant is illustrated by the sequence of lines constructed for appropriately chosen values of the cosmological parameter λ.

In polytropes with $n > 0$, the binding energy E_b differs from the gravitational binding energy $(-\mathcal{G})$, as some of the work of the gravitational field is converted into the kinetic energy of microscopic motion in these polytropes. The role of the cosmological parameter $\lambda > 0$ in the effect of gravitational binding will be discussed in the next section.

VII. GRPS WITH THE COSMOLOGICAL CONSTANT

We construct models of the GRPs with $n > 0$ and discuss their dependence on the cosmological parameter λ. We present the length and mass scales of the polytropes and determine the existence restrictions put on the parameters characterizing their structure. Then, we discuss the polytrope global characteristics as the dimensionless mass and dimensionless radius, compactness, and gravitational and binding energy of the polytrope configuration. Finally, we study the radial profiles of the energy density, pressure, and metric coefficients and illustrate the polytrope curvature by embedding diagrams of the ordinary projected geometry and the optical geometry.

A. Length scale and mass scale

The polytropic spheres are determined by the dimensionless structure equations that are governed by three parameters—the polytropic index n, the relativistic parameter σ, and the cosmological parameter λ—and by the central density ρ_c governing, simultaneously with the parameters n, σ, the dimensional length and mass scale of the polytropic spheres. The dimensional length and mass scales are given by the respective relations

$$\mathcal{L} = 3.27\frac{[\sigma(n+1)]^{1/2}}{\rho_c^{1/2}}(10^{13}\ \mathrm{cm}), \tag{132a}$$

$$\mathcal{M} = 4.41\frac{[\sigma(n+1)]^{3/2}}{\rho_c^{1/2}}(10^{41}\ \mathrm{g}); \tag{132b}$$

ρ_c has to be substituted in units of $\mathrm{g/cm^3}$. The polytropic spheres with given mass and length scales are determined by solutions of the structure equations that are governed by

the dimensionless radial coordinate $\xi_1(n,\sigma,\lambda)$ and the related dimensionless mass parameter $v(\xi_1)(n,\sigma,\lambda)$.

B. Integration of the structure equations

The differential structure equations have to be solved numerically for any polytropic index $n > 0$. For each fixed value of n, we obtain a sequence of polytropic spheres determined by the central density ρ_c, the relativistic parameter σ, and the cosmological parameter λ. For the observationally fixed value of the repulsive cosmological constant, $\Lambda = 1.3 \times 10^{-56}$ cm^{-2}, and the related vacuum energy density, ρ_{vac}, the central density of the polytrope, ρ_c, governs the value of the cosmological parameter λ, and it is not a free parameter in such a situation. The first (lowest) solution ξ_1 of the equation $\theta(\xi) = 0$ determines the extension of the polytropic spheres in terms of the dimensionless radius ξ; their dimensional radius reads $R = \mathcal{L}\xi_1$. The dimensionless mass parameter is given by $v(\xi_1) = v_1$, and the polytrope gravitational mass is then given by $M = \mathcal{M}v(\xi_1)$. The radial profiles of the energy density, pressure, gravitational mass parameter, and the metric coefficients are determined by the functions $\rho(\xi;n,\sigma,\lambda)$, $p(\xi;n,\sigma,\lambda)$, $v(\xi;n,\sigma,\lambda)$, $g_{tt}(\xi;n,\sigma,\lambda)$, and $g_{rr}(\xi;n,\sigma,\lambda)$—note that the metric coefficients depend on ξ also through the mass parameter $v(\xi)$. These functions are given by Eqs. (38) and (39). In a similar way, the embedding diagrams of the ordinary and optical geometry are given by the functions $z_{ord}(\xi;n,\sigma,\lambda)$ and $z_{opt}(\xi g_{tt}^{1/2};n,\sigma,\lambda)$. It is also instructive to illustrate the dependence of the other global characteristics of the polytropic spheres on the basic parameters, i.e., the functions of compactness $\mathcal{C}(\xi = \xi_1;n,\sigma,\lambda)$, the gravitational potential energy $\mathcal{G}(\xi = \xi_1;n,\sigma,\lambda)$, and the binding energy of the polytropic gas $E_b(\xi = \xi_1;n,\sigma,\lambda)$.

C. Limit on existence of the GRPs

We have found the role of the cosmological parameter λ as being concentrated in putting strong limits on the existence of polytropic spheres in dependence on both the polytropic index n and the relativistic parameter σ. The critical, limiting values of the cosmological parameter, given by the function $\lambda_{crit} = \lambda_{crit}(n;\sigma)$, have been determined by numerical calculations and are represented for selected representative values of n in Fig. 3; the polytropes are allowed at regions of the parameter space below the critical curves. We cover the range of standard values of the polytropic index, starting at the nonrelativistic fluid with $n = 3/2$ and finishing at $n = 3$ for the ultrarelativistic fluid, and we add both some values of $n < 3/2$, and some values of $n > 3$ when a special character of the polytrope properties occurs. Extension of the critical curves is restricted by the value of the relativistic parameter σ corresponding to the equality of the velocity of sound and the velocity of light (so-called causality limit).

We can see that the character of the critical function $\lambda_{crit}(n,\sigma)$ strongly depends on the value of the polytropic index n. Generally, it increases with n decreasing. For $n < 3$, the function $\lambda_{crit}(n;\sigma)$ slightly monotonically decreases with σ increasing; it is limited by the value of $\lambda_{crit} = 10^{-7}$ even in the limit of $\sigma \to 1$. In the special case of

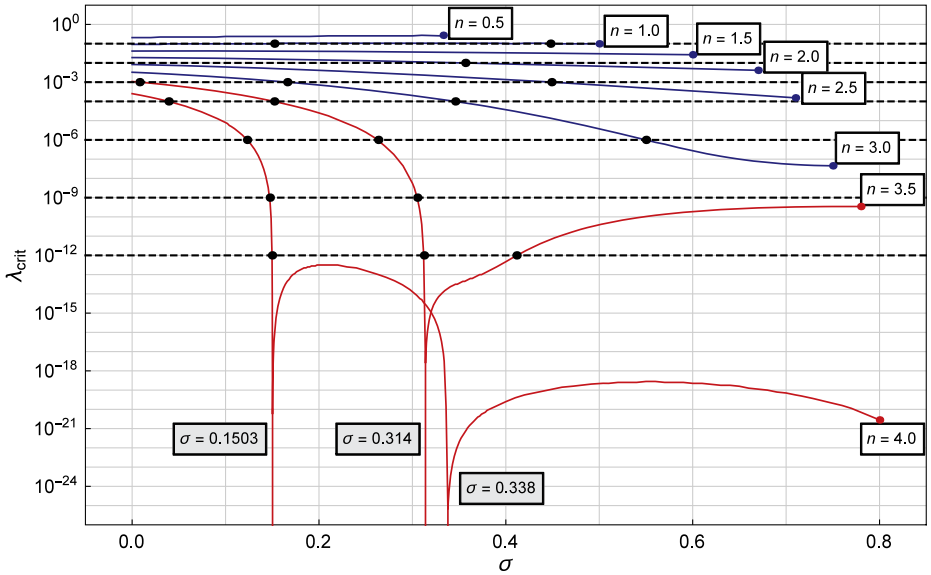

FIG. 3. Dependence of the critical value of the cosmological parameter on the relativity parameter σ for the polytropic index taken from 0.5 to 4.0 with step of 0.5. For a particular polytropic index, the polytropic configurations can only exist for parameter points (σ,λ) located below the corresponding curve. For polytropic configurations with $n \leq 3.34$, critical values of the relativistic parameter, σ_f, exist, giving infinitely extended configurations [141]. For polytropes with $n = 3.5$, one such critical point is relevant, while for polytropes with $n = 4$, two such points are relevant.

$n = 3$, it decreases from the starting point $\lambda_{\rm crit}(n = 3, \sigma = 0) = 3 \times 10^{-3}$ down to $\lambda_{\rm crit}(n = 3; \sigma = 0.7) = 10^{-7}$ and remains constant with increasing values of σ.

For $n > 3$, the function $\lambda_{\rm crit}(n; \sigma)$ loses its monotonic character, and there are forbidden polytropes for some special values of the relativistic parameter σ in dependence on the polytrope index, since such polytropes should have infinite extension. For example, for $n = 3.5$ the polytropes are forbidden for one specific value of $\sigma_{\rm f} = 0.314$, while for $n = 4$, there are two specific forbidden values of $\sigma_{\rm f1} = 0.1503$, $\sigma_{\rm f2} = 0.338$. A third forbidden configuration with $n = 4$ corresponds to σ breaking the causality limit and reads $\sigma_{\rm f3} = 0.834$. These forbidden configurations occur for the general relativistic polytropic configurations in the spacetimes with $\Lambda = 0$ and were discussed for the first time in Refs. [123].

Notice that in the region of $\sigma > \sigma_{\rm f1}$ there is $\lambda_{\rm crit}(n; \sigma) < 10^{-10}$. On the other hand, for nonrelativistic polytrope spheres with $\sigma < 0.1$, there is $\lambda_{\rm crit}(n; \sigma) > 10^{-5}$ for all polytropic indexes $n < 4$. In such situations, we can

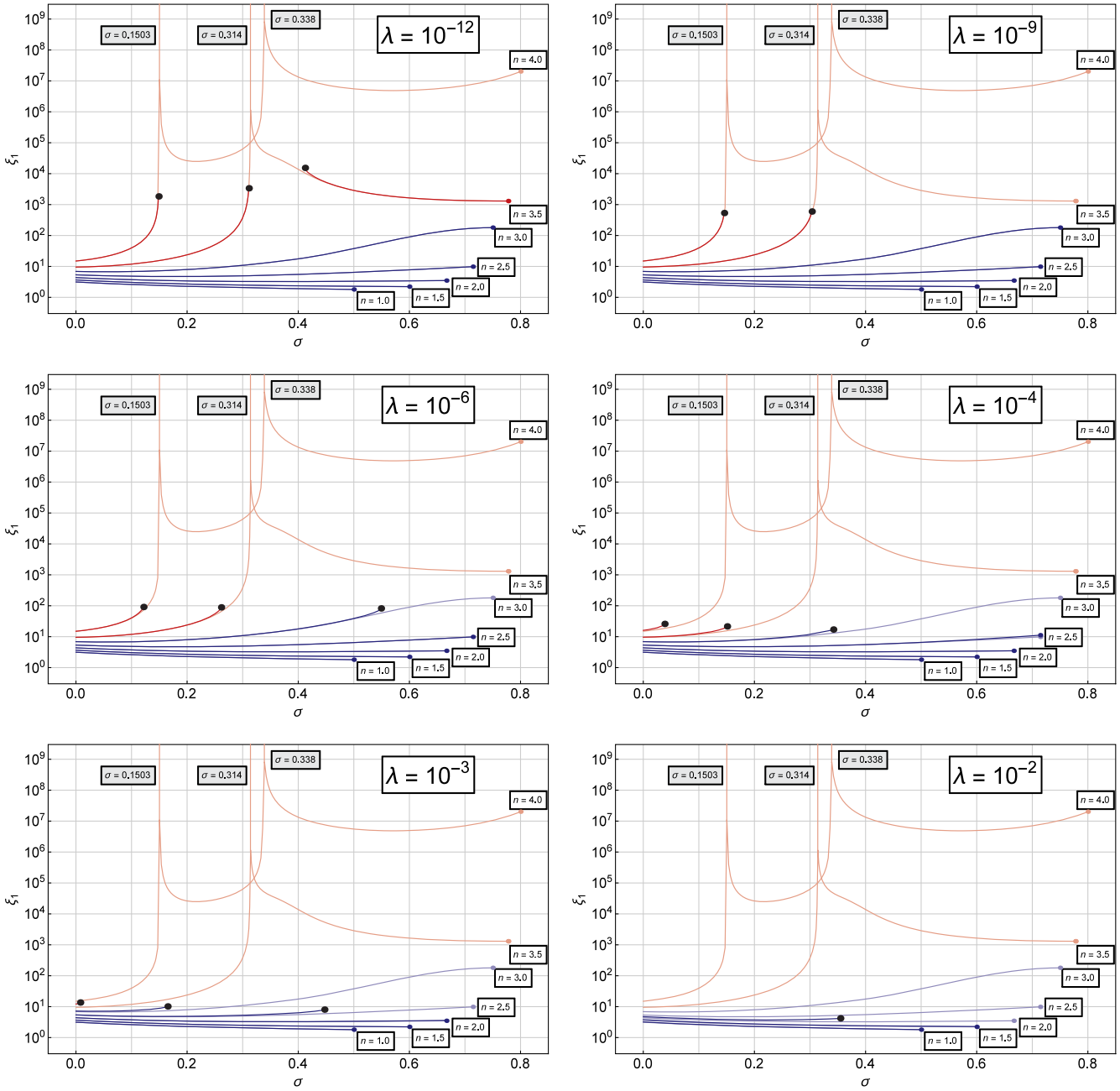

FIG. 4. Dependences of the extension parameter ξ_1 for the characteristic values of the polytropic index $n \in \{1.0, 1.5, 2, 2.5, 3, 3.5, 4\}$ with σ varying up to the causal limit for $\lambda = 10^{-12}$, $\lambda = 10^{-9}$ (top); $\lambda = 10^{-6}$, $\lambda = 10^{-4}$ (middle); and $\lambda = 10^{-3}$, $\lambda = 10^{-2}$ (bottom).

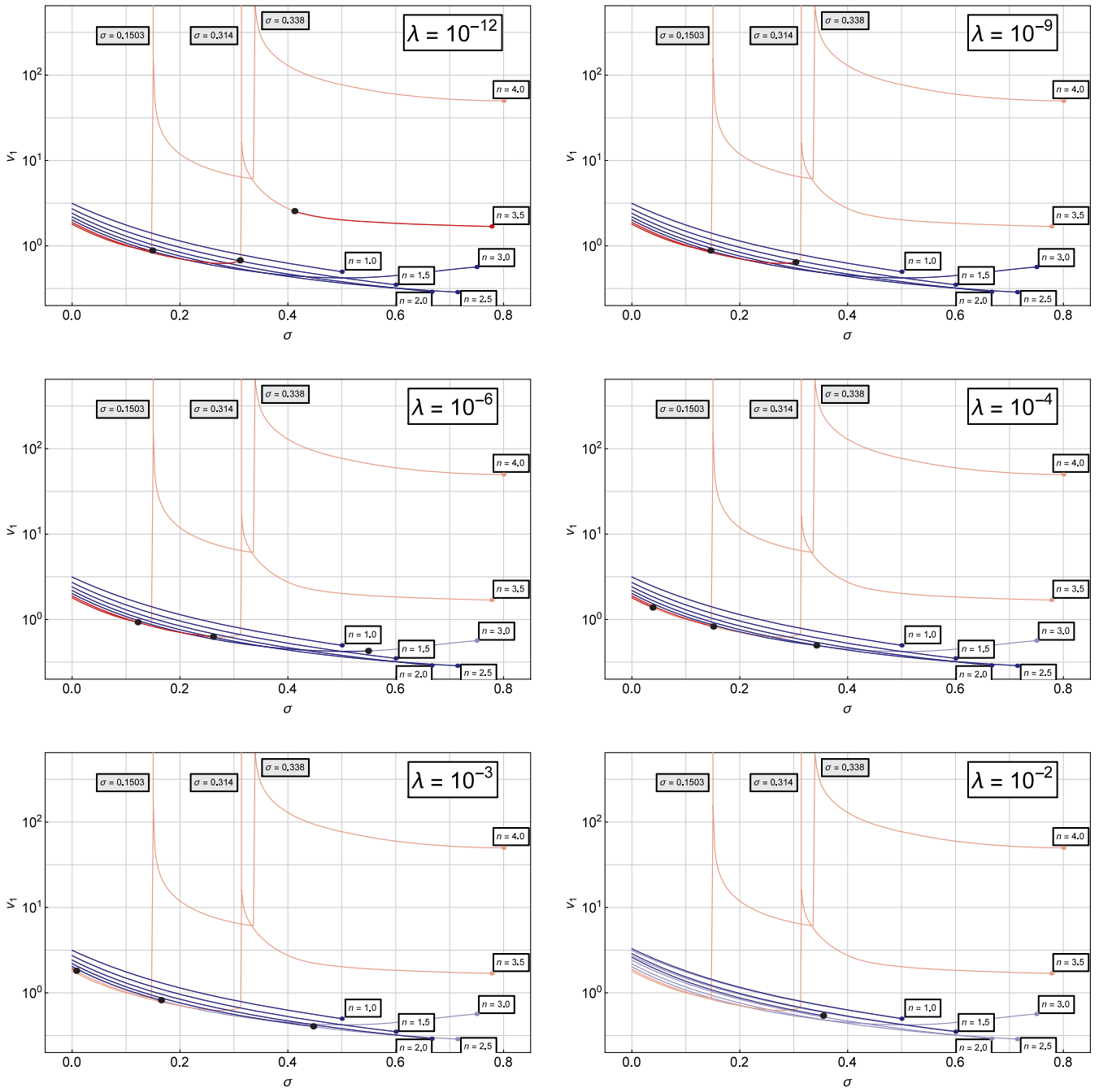

FIG. 5. Dependences of the mass parameter $v_1 \equiv v(\xi_1)$ for the characteristic values of the polytropic index $n \in \{1.0, 1.5, 2, 2.5, 3, 3.5, 4\}$ with σ varying up to the causal limit for $\lambda = 10^{-12}$, $\lambda = 10^{-9}$ (top); $\lambda = 10^{-6}$, $\lambda = 10^{-4}$ (middle); and $\lambda = 10^{-3}$, $\lambda = 10^{-2}$ (bottom).

see that the polytropic spheres with very small central density have their structure strongly influenced by the repulsive cosmological constant.

VIII. GLOBAL GRP CHARACTERISTICS

A. Extension and mass

The basic global characteristics of the GRPs are given by the dimensionless extension and dimensionless mass. We thus give dependences of the polytrope extension parameter ξ_1 and the polytrope mass parameter $v_1 = v(\xi_1)$ on the parameters n, σ, and λ and discuss their properties.

We first illustrate dependences of the extension parameter ξ_1 for the characteristic values of the polytropic index $n = 1$, 1.5, 2, 2.5, 3, 3.5, 4, with σ varying up to the causal limit. The dependence of the dimensionless radius of the polytropes on the cosmological constant parameter λ is presented in Fig. 4 where we vary the cosmological

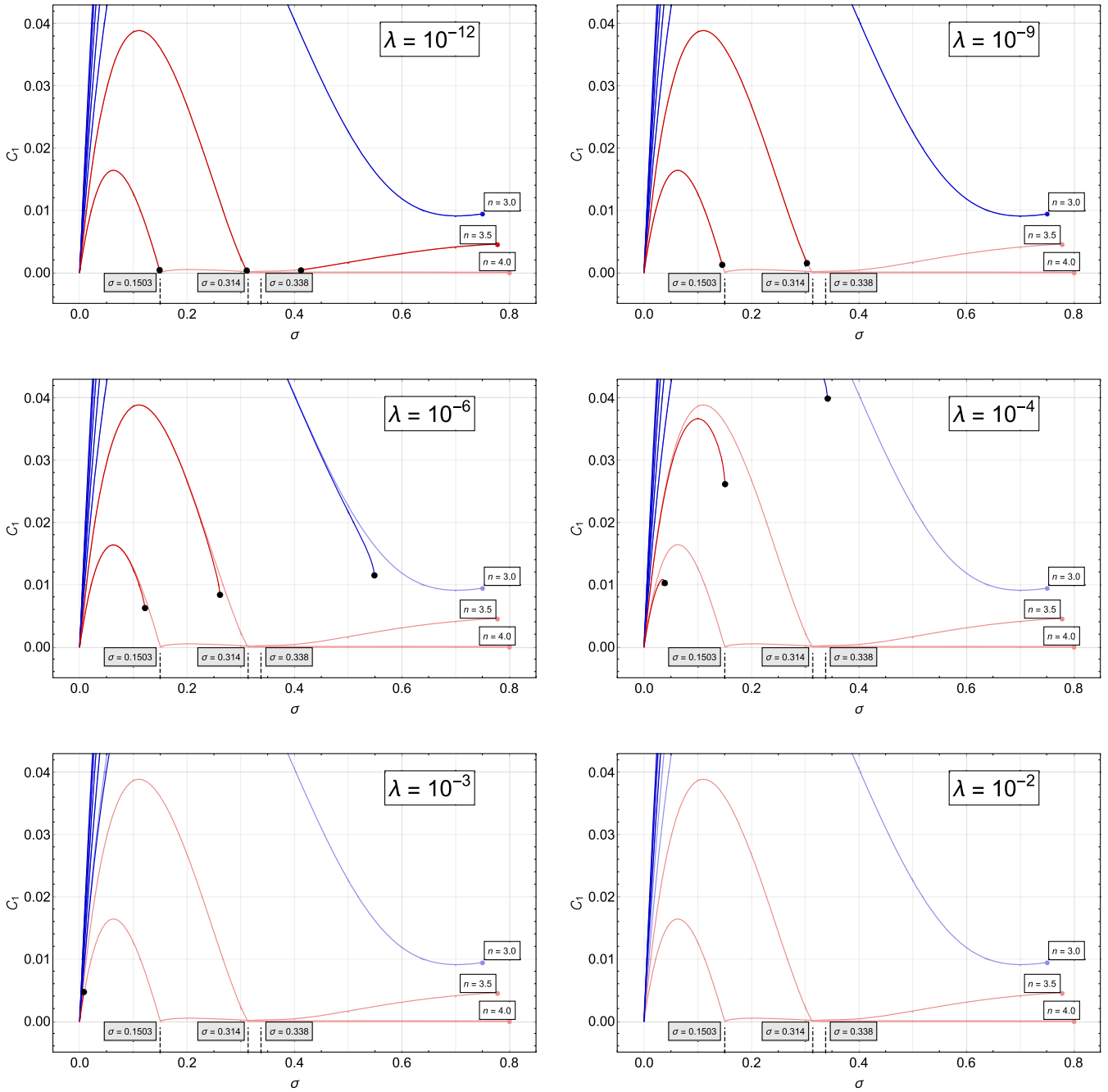

FIG. 6. Dependences of the compactness $\mathcal{C}_1$ for the characteristic values of the polytropic index $n \in \{1.0, 1.5, 2, 2.5, 3, 3.5, 4\}$ with σ varying up to the causal limit for $\lambda = 10^{-12}$, $\lambda = 10^{-9}$ (top); $\lambda = 10^{-6}$, $\lambda = 10^{-4}$ (middle); and $\lambda = 10^{-3}$, $\lambda = 10^{-2}$ (bottom).

parameter for the characteristic values of $\lambda = 10^{-12}$, 10^{-9}, 10^{-6}, 10^{-4}, 10^{-3}, 10^{-2}. The curves $\xi_1(\sigma, n, \lambda)$ are compared to the curves $\xi_1(\sigma, n, \lambda = 0)$—we can see that at the critical points of σ_f the dimensionless parameter ξ_1 diverges for $\lambda = 0$, indicating that the critical polytrope cannot be limited and is not well defined. The validity restriction of the curves $\xi_1(\sigma, n, \lambda)$ at the causal limit is depicted by the shaded points. The black points depict the limit of validity of the curves $\xi_1(\sigma, n, \lambda)$ meaning that the polytrope radius cannot exceed the static radius of the external spacetime.

Then, we illustrate dependences of the mass parameter $v_1 = v(\xi_1)$ for the same characteristic values of the polytropic index $n = 1$, 1.5, 2, 2.5, 3, 3.5, 4, with σ varying up to the causal limit. The dependence of the dimensionless mass parameter of the polytropes on the cosmological constant parameter λ is presented in Fig. 5, where we again vary the parameter for the characteristic values of $\lambda = 10^{-12}$, 10^{-9}, 10^{-6}, 10^{-4}, 10^{-3}, 10^{-2}. In Fig. 5, the curves $v_1(\sigma, n, \lambda)$ are compared to the curves $v_1(\sigma, n, \lambda = 0)$. At the critical points of σ_f, the

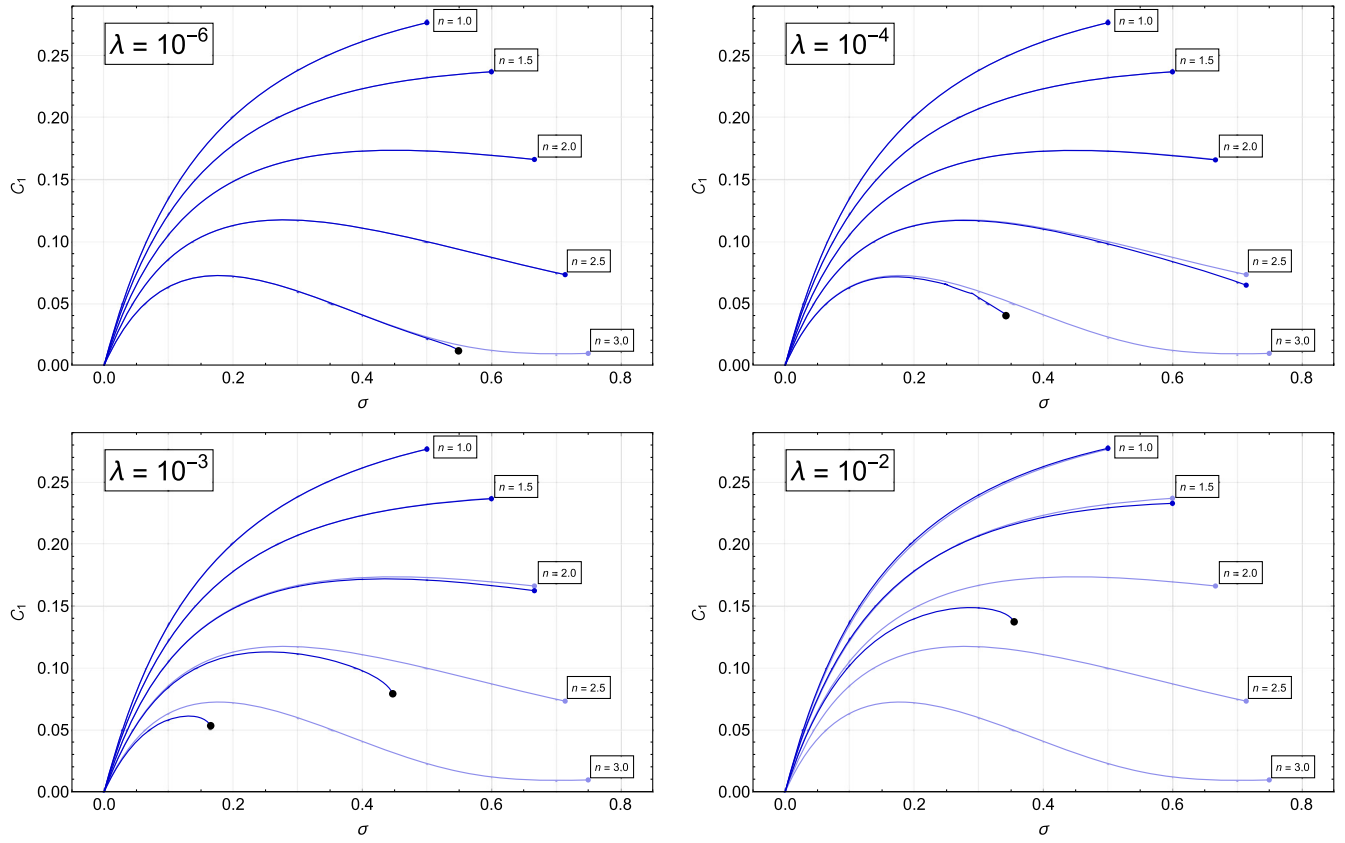

FIG. 7. Extended dependences of the compactness $\mathcal{C}_1$ for the characteristic values of the polytropic index $n \in \{1.0, 1.5, 2, 2.5, 3, 3.5, 4\}$ with σ varying up to the causal limit for $\lambda = 10^{-6}$, $\lambda = 10^{-4}$ (top) and $\lambda = 10^{-3}$, $\lambda = 10^{-2}$ (bottom). For $n \leq 3$, the compactness $\mathcal{C}_1$ σ profiles are illustrated for the whole existence ranges, extending thus the detailed picture given in Fig. 6.

dimensionless parameter v_1 also diverges for $\lambda = 0$ and even faster than for the dimensionless radius, indicating again that the critical polytrope has to be unlimited and is not well defined for $\lambda = 0$. The causal limit of validity of the curves $v_1(\sigma, n, \lambda)$ is depicted by the shaded points.

1. Extension parameter

For $\lambda = 0$, the polytropes with $\sigma \ll 1$ have the dimensionless radius $\xi_1 \sim 1$, and it slightly increases with increasing n. With increasing σ, the radius ξ_1 slightly decreases for $n = 3/2$, it remains almost constant for $n = 2$, and it has a minimum near $\sigma \sim 0.1$ and then increases up to values of $\xi_1 = 10$ for $n = 2.5$ and $\xi_1 \sim 200$ for $n = 3$. For $n = 3.5$, ξ_1 diverges at $\sigma_f = 0.314$, and then it decreases to $\xi_1 \sim 10^3$ at the causal limit. For $n = 4$, the radius ξ_1 diverges at the two critical points; between the critical points, there is $\xi_1 > 10^4$; and at the causal limit, there is $\xi_1 \sim 3 \times 10^7$.

The cosmological constant has a crucial influence on the polytropic configurations, as it removes the singular behavior of ξ_1—for any value of $\lambda > 0$, the polytropes with $n = 3.5$ or $n = 4$ are forbidden around the critical values of σ_f.

For $\lambda = 10^{-12}$, the restriction implies $\xi_1 < 10^4$ for all values of polytrope index n. For $n = 4$, the branch of $\xi_1(\sigma)$ above the first critical point is forbidden, while for $n = 3.5$, the polytropes can exist both above and below the critical values of σ_f. For $n \leq 3$, the influence of $\lambda > 0$ in the functions $\xi_1(\sigma; n, \lambda)$ is negligible—see the top-left plot in Fig. 4.

A similar situation occurs for $\lambda = 10^{-9}$, but for $n > 3$, the polytropes exist only under the critical value of the first σ_f. The functions $\xi_1(\sigma; n, \lambda)$ are smaller than 10^3, and as in the previous case, they follow closely those corresponding to $\lambda = 0$ (see the top-right plot in Fig. 4).

For $\lambda = 10^{-6}$, the functions $\xi_1(\sigma; n, \lambda)$ with $n = 3, 3.5, 4$ have their terminal point at the same value of $\xi_1 \sim 10^2$ with the terminal value of σ increasing with decreasing n; now, the influence of $\lambda > 0$ slightly increases the $\xi_1(\sigma; n, \lambda)$ functions above their counterparts with $\lambda = 0$ (see the middle-left plot in Fig. 4).

A similar situation occurs for $\lambda = 10^{-4}$, but in this case, $\xi_1(\sigma, n) < 30$ (middle-right plot in Fig. 4).

For $\lambda = 10^{-3}$, the $n = 4$ polytropes are fully suppressed, the $n = 3.5$ polytropes are allowed at vicinity of $\sigma = 0$ only, while for $n = 3$ ($n = 2.5$), the polytropes are limited at

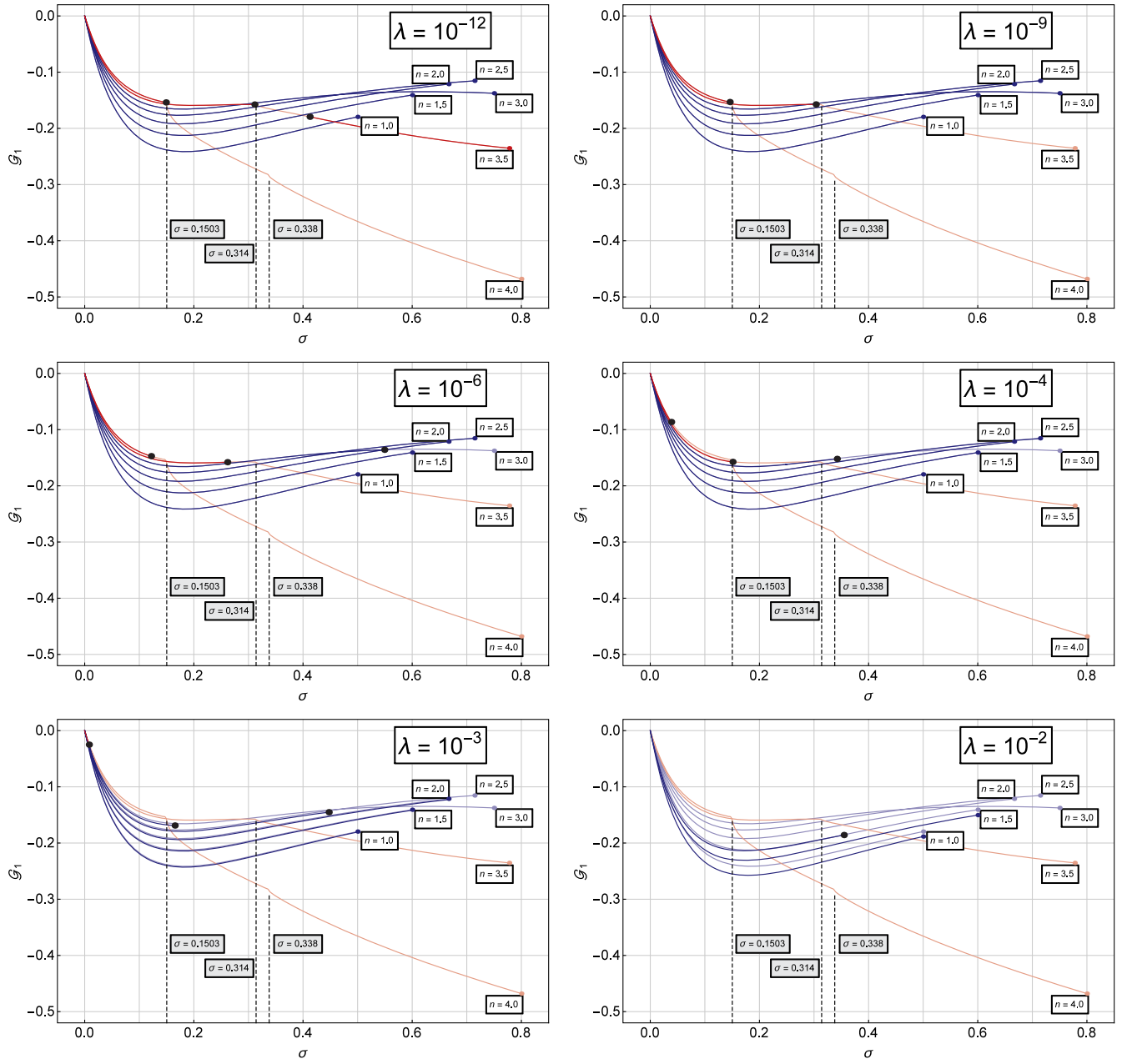

FIG. 8. Dependences of the gravitational energy $\mathcal{G}_1$ for the characteristic values of the polytropic index $n \in \{1.0, 1.5, 2, 2.5, 3, 3.5, 4\}$ with σ varying up to the causal limit for $\lambda = 10^{-12}$, $\lambda = 10^{-9}$ (top); $\lambda = 10^{-6}$, $\lambda = 10^{-4}$ (middle); and $\lambda = 10^{-3}$, $\lambda = 10^{-2}$ (bottom).

$\sigma \sim 0.15$ ($\sigma \sim 0.45$), and the functions $\xi_1(\sigma, n, \lambda) < 10$ demonstrating slight influence of $\lambda > 0$ for σ near the maximal allowed values; for the polytropes with $n = 2$, 1.5, 1, the influence of the cosmological constant is negligible—see the bottom-left plot in Fig. 4.

For $\lambda = 10^{-2}$, only the polytropes with $n \leq 2$ are allowed. The limiting value of the relativistic parameter is shifted down to $\sigma \sim 0.35$ in the case of $n = 2$ polytropes, while it is not influenced by the cosmological constant for polytropes $n = 1.5$, 1; generally, the functions $\xi_1(\sigma, n, \lambda) < 8$, and their σ profile is influenced by the cosmological constant only for $n = 2$—see the bottom-right plot in Fig. 4.

2. Mass parameter

For $\lambda = 0$, polytropes with $\sigma \ll 1$ have the dimensionless mass parameter $v_1 = v(\xi_1) \sim 1$, decreasing from $v_1 \sim 2.75$ for $n = 1.5$ down to $v_1 \sim 2$ for $n = 4$. For $n = 1.5$, 2.2.5, the function $v_1(\sigma, n)$ decreases with increasing σ, down to values $v_1 \sim 0.25$ near the causal limit. For $n = 3$, $v_1(\sigma, n)$ has a minimum at $\sigma \sim 0.45$ and then slightly increases with σ increasing to the causality limit.

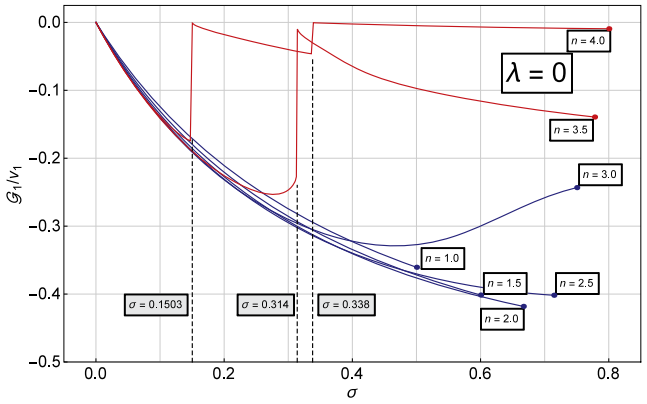

FIG. 9. Dependences of the relative gravitational energy $\mathcal{G}_1/v_1$ for the characteristic values of the polytropic index $n \in \{1.0, 1.5, 2, 2.5, 3, 3.5, 4\}$ with σ varying up to the causal limit for $\lambda = 0$.

For $n = 3.5$, 4, the mass parameter of the polytropes demonstrates again divergence at the critical points σ_f. At the causal limits, the mass parameter takes the value of $v_1 \sim 2$ ($v_1 \sim 30$) for $n = 3.5$ ($n = 4$).

Similarly to the case of the extension parameter ξ_1, the role of the cosmological constant represented by the parameter λ in the mass parameter function $v_1(\sigma, n, \lambda)$ is given by the cutoffs governed by the existence limits on the GRPs determined in Fig. 3. The cutoffs are illustrated in Fig. 5 for the same values of the parameter λ as in the case of the extension parameter ξ_1. Now, we can see that in the regions of validity the functions $v_1(\sigma, n, \lambda)$ almost coincide with the functions $v_1(\sigma, n, \lambda = 0)$. Notice that, even for $\lambda = 10^{-12}$, the mass parameter $v_1(\sigma, n) < 3$ for all considered values of n and in the whole allowed region of σ. Large values of the mass parameter $v_1(\sigma, n, \lambda)$, say $v_1 > 10^4$, can be obtained for GRPs with $n = 3.5$, 4 in the vicinity of the critical values of σ_f, if $\lambda < 10^{-17}$.

3. Compactness

Compactness is defined as the dimensionless ratio of the mass and extension of the polytrope; i.e., it is governed by the ratio v_1/ξ_1. As we consider here the global compactness parameter, related to the complete polytropic configurations given by the parameters ξ_1 and v_1, we use the notation $\mathcal{C}_1 = \mathcal{C}(\xi_1)$. Later, we study also the radial profiles of the compactness $\mathcal{C}(\xi)$, defined for $\xi \in (0, \xi_1)$ with related $v(\xi)$.

The influence of the cosmological constant on the compactness function $\mathcal{C}_1(n; \sigma, \lambda)$ of the GRPs is represented in Figs. 6 and 7 for the same values of the polytrope index n and the dimensionless parameter λ as in the case of ξ_1 and v_1.

All the functions are compared to the compactness function $\mathcal{C}_1(n; \sigma, \lambda = 0)$ for the same values of the polytropic index n. There is $\mathcal{C}(n; \sigma = 0, \lambda) = 0$ for all values of the cosmological parameter λ allowing the existence of the static polytropes. In the case of $\lambda = 0$, we can see that for $n = 1.5$ the compactness parameter increases with increasing relativistic parameter σ reaching the largest value of $\mathcal{C}_1 \sim 0.235$ at the causality limit. For $n = 2$, 2.5, 3, the compactness parameter $\mathcal{C}_1$ reaches a maximal value in the middle of the interval of allowed values of σ and then decreases to a minimum at the causality limit of σ. The σ profile of the compactness parameter strongly decreases with increasing polytropic index n—for $n = 2$, there is $\mathcal{C}_1 < 0.175$, while for $n = 3$, there is $\mathcal{C}_1 < 0.1$. For the polytropes with $n = 3.5$, 4, demonstrating the divergent behavior of the extension parameter ξ_1 at the critical values of σ_f, the σ profile of the compactness parameter contains zero points at the critical points σ_f, reaching a maximum between $\sigma = 0$ and σ_f points. The compactness parameter $\mathcal{C}_1$ significantly decreases with increasing n. For $n = 3.5$, there is $\mathcal{C}_1 < 0.04$, while $\mathcal{C}_1 < 0.17$ for $n = 4$ polytropes. Notice that in the case of the $n = 4$ polytropes there is $\mathcal{C}_1 < 10^{-4}$ for $\sigma > \sigma_{f2}$—polytropes with such extremely low compactness parameter $\mathcal{C}_1$ occur, as their extension parameter ξ_1 has to be extremely high.

In the case of the compactness parameter function $\mathcal{C}_1(n; \sigma, \lambda)$, the role of the repulsive cosmological constant is again concentrated in the cutoff of the polytropes allowed for fixed parameters n and σ, when strong restrictions appear with n increasing. Further, we can observe in Figs. 6 and 7 significant modifications of the σ profile in addition to the limits implied by the restriction on the existence of the polytropic equilibrium configurations. The modifications of the $\mathcal{C}_1(n; \sigma, \lambda)$ σ profiles become substantial for $\lambda \geq 10^{-6}$, and the influence of the cosmological constant always decreases compactness of the polytrope while the other parameters are kept fixed.

B. Energy of polytropes

We can appropriately describe the GRPs by global characteristics reflecting the result of interplay of the gravitational forces and the forces governing properties of matter constituting the polytrope. We consider now the representative global characteristics, gravitational energy, and binding energy of the complete equilibrium polytropic configurations characterized by parameters ξ_1 and v_1. We thus denote them as $\mathcal{G}_1 = \mathcal{G}(\xi_1)$ for the gravitational energy and $\mathcal{B}_1 = \mathcal{B}(\xi_1)$ for the binding energy. Later, we shall consider also their radial profiles $\mathcal{G}(\xi)$ and $\mathcal{B}(\xi)$.

1. Gravitational energy

The dimensionless gravitational energy $\mathcal{G}_1$ represents a global characteristic of binding effects of gravity in equilibrium and has to be negative for any polytrope. The role of the cosmological constant in the behavior of the gravitational energy of the polytropes is represented in Fig. 8 for the same values of the polytrope index n and the dimensionless parameter λ as in the case of quantities ξ_1

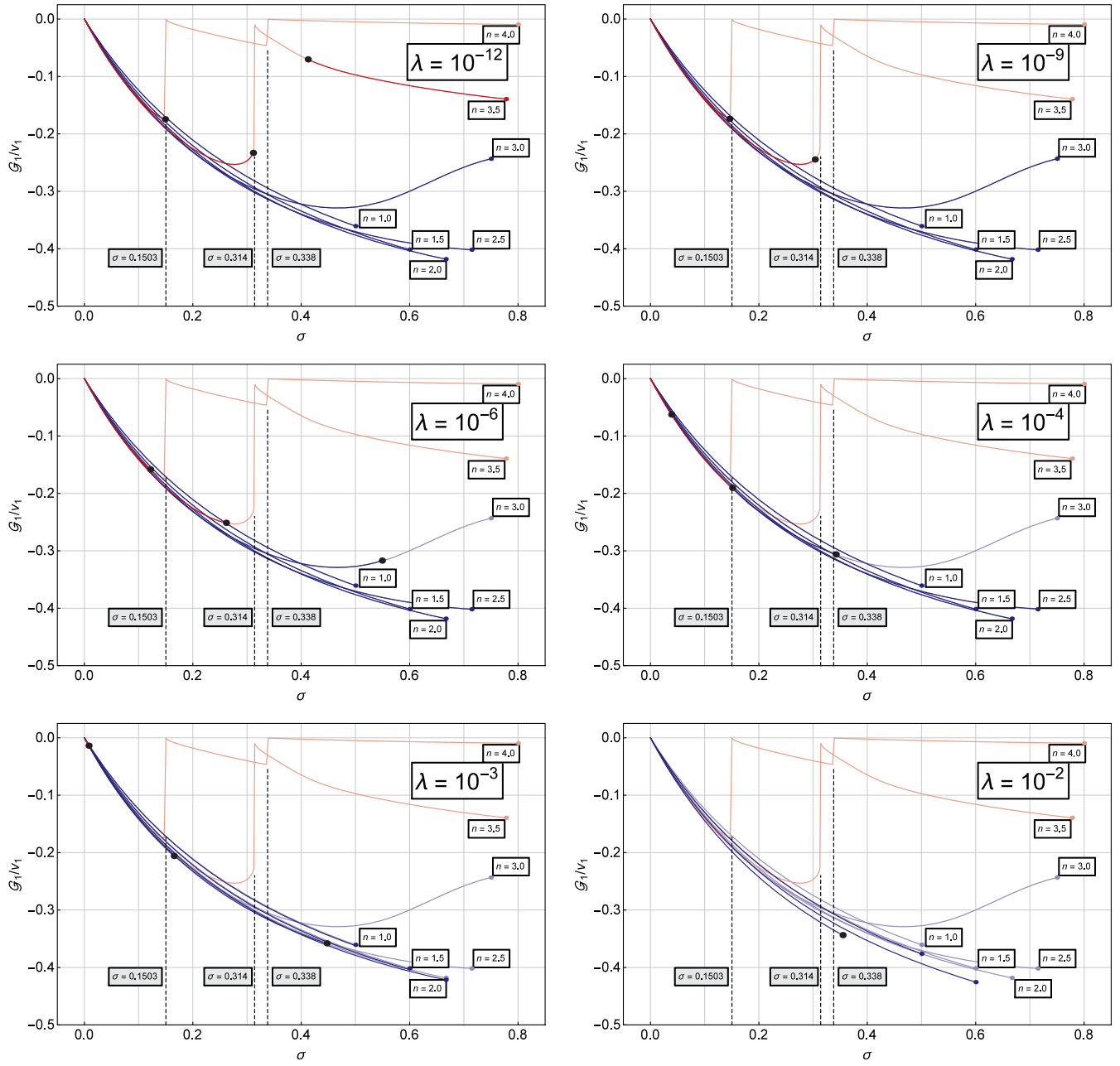

FIG. 10. Dependences of the relative gravitational energy $\mathcal{G}_1/v_1$ for the characteristic values of the polytropic index $n \in \{1.0, 1.5, 2, 2.5, 3, 3.5, 4\}$ with σ varying up to the causal limit for $\lambda = 10^{-12}$, $\lambda = 10^{-9}$ (top); $\lambda = 10^{-6}$, $\lambda = 10^{-4}$ (middle); and $\lambda = 10^{-3}$, $\lambda = 10^{-2}$ (bottom).

and v_1. The gravitational energy function $\mathcal{G}_1(n;\sigma,\lambda)$ is always compared to the function $\mathcal{G}_1(n;\sigma,\lambda=0)$. In the case of $\lambda = 0$, there is $\mathcal{G}_1(n;\sigma=0) = 0$, and the gravitational energy of polytropes with $n = 1.5$, 2, 2.5 reaches a minimal value in the middle of the interval of allowed values of the relativistic parameter σ and then increases to a maximum at the causality limit on the value of σ. In the case of $n = 3$ polytropes, the σ profile of the gravitational energy has a maximum following the minimum. At the minimum of the σ profile, the gravitational energy significantly decreases with decreasing polytropic index n (gravitational binding increases), demonstrating a shift from the value of $\mathcal{G}_1 \sim -0.17$ in the case $n = 3$ to the value of $\mathcal{G}_1 \sim -0.21$ in the case $n = 1.5$. For the polytropes with $n = 3.5$, 4, having the divergence of ξ_1 at the critical values of σ_f, the σ profile of the gravitational energy is continuous at the critical points, but its derivative has a jump there. In the region of large values of σ, the gravitational energy demonstrates a strong decrease, and in the case of the $n = 4$ polytropes, $\mathcal{G}_1 \sim -0.47$ at the causality limit, demonstrating thus strong gravitational binding.

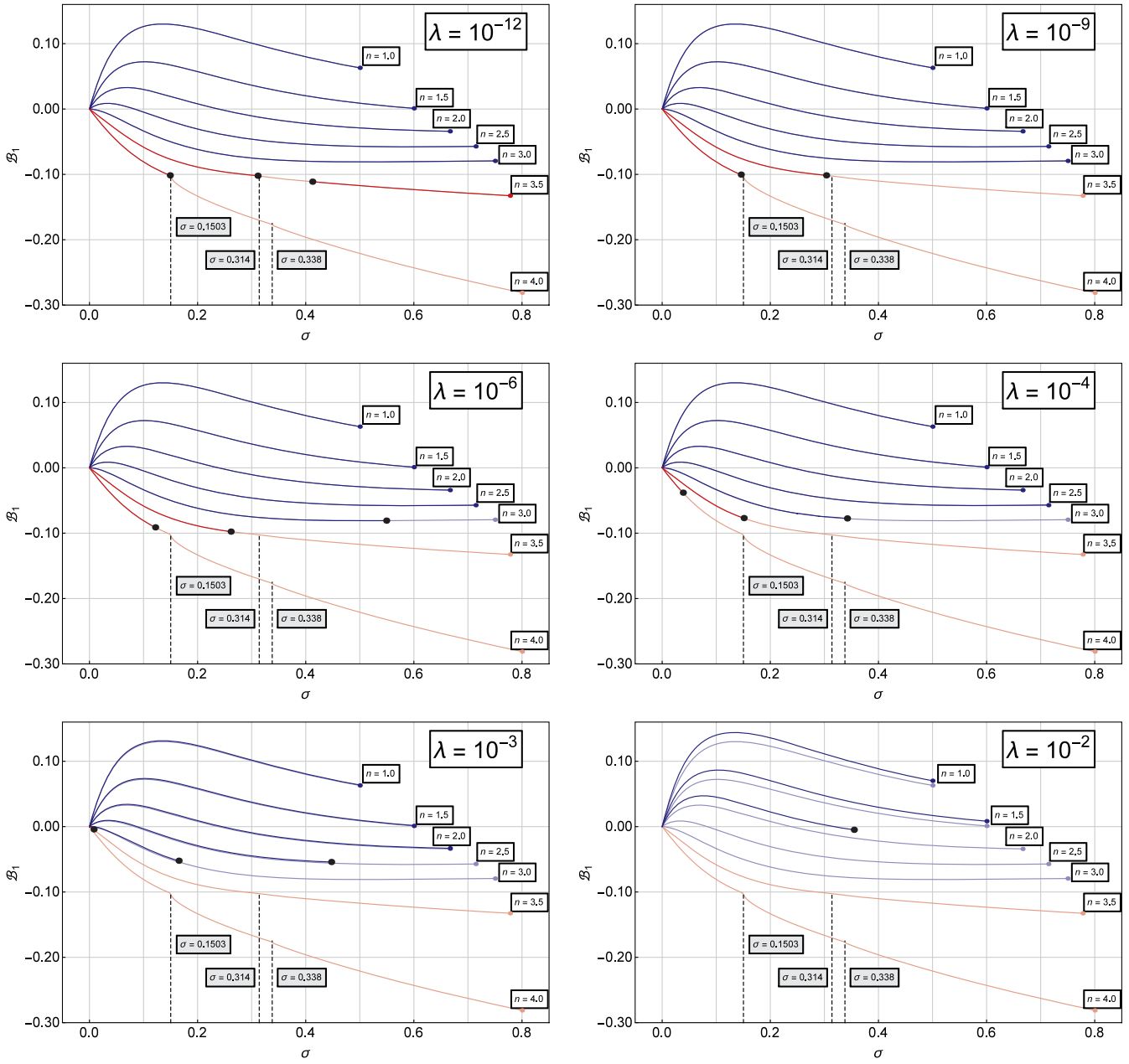

FIG. 11. Dependences of the binding energy $\mathcal{B}_1$ for the characteristic values of the polytropic index $n \in \{1.0, 1.5, 2, 2.5, 3, 3.5, 4\}$ with σ varying up to the causal limit for $\lambda = 10^{-12}$, $\lambda = 10^{-9}$ (top); $\lambda = 10^{-6}$, $\lambda = 10^{-4}$ (middle); and $\lambda = 10^{-3}$, $\lambda = 10^{-2}$ (bottom).

For $\mathcal{G}_1(n;\sigma,\lambda)$, Fig. 8 demonstrates that the role of the cosmological constant parameter is again reflected mainly by the cutoff in allowed values of the parameter σ for polytropes with fixed parameter n—strong restrictions occur with n increasing, in similarity with the previously considered cases. We can also observe a slight modification of the σ profile in addition to the limits implied by the restriction on the existence of the polytropic equilibrium configurations. However, modifications of the $\mathcal{G}_1(n;\sigma,\lambda)$ σ profiles large enough to be recognized occur only for $\lambda \geq 10^{-3}$—increasing λ always decreases the gravitational energy of the polytrope, while other parameters are fixed.

For completeness, we give also the σ profiles for the relative gravitational energy defined as $\mathcal{G}_1/v_1(n;\sigma,\lambda)$; i.e., the gravitational energy is related to the dimensionless gravitational mass of the polytrope. There is $\mathcal{G}/v_1(n;\sigma=0)=0$. For $\lambda = 0$, the relative gravitational energy $\mathcal{G}_1/v_1(n;\sigma,\lambda=0)$ is illustrated in Fig. 9. We can see that the character of the σ profiles for polytropes with $n = 1$, 1.5, 2, 2.5, 3 is the same as for the gravitational energy, but its magnitude is larger than for the gravitational energy. On the other hand, a substantial change occurs in the $\mathcal{G}_1/v_1$ σ profiles of the $n = 3.5, 4$ polytropes, as a jump to a zero point has to occur at the critical points

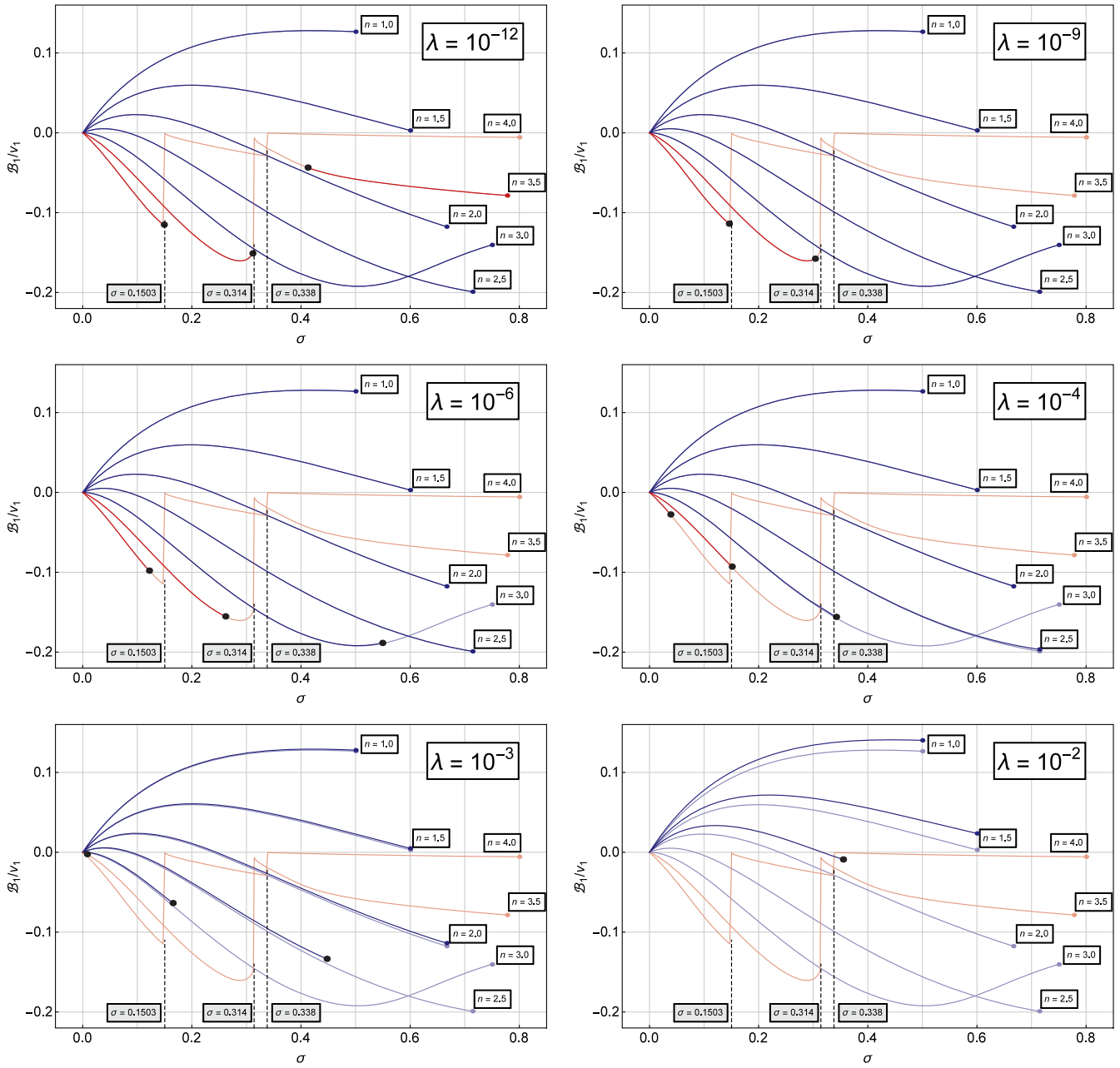

FIG. 12. Dependences of the relative binding energy $\mathcal{B}_1/v_1$ for the characteristic values of the polytropic index $n \in \{1.0, 1.5, 2, 2.5, 3, 3.5, 4\}$ with σ varying up to the causal limit for $\lambda = 10^{-12}$, $\lambda = 10^{-9}$ (top); $\lambda = 10^{-6}$, $\lambda = 10^{-4}$ (middle); and $\lambda = 10^{-3}$, $\lambda = 10^{-2}$ (bottom).

of relativistic parameter σ_f due to the behavior of v_1, and the profiles of the $n = 3.5$, 4 polytropes are located above the profiles of polytropes with lower n at the region of large values of σ, contrary to the case of gravitational energy.

The influence of the cosmological constant on the σ profiles of the relative gravitational energy $\mathcal{G}_1/v_1(n;\sigma,\lambda)$ is illustrated in Fig. 10. We can see that for polytropes with fixed parameter n the influence is represented mainly by the cutoff at the allowed values of the parameter σ, while the modifications of the profiles due to the nonzero λ term are very small, and they decrease the global parameter $\mathcal{G}_1/v_1$ of the GRPs.

2. Binding energy

The dimensionless binding energy $\mathcal{B}_1$ represents the combination of the binding effects of gravity and the internal energy of the polytrope. It can be thus positive or negative, according to domination of negative gravitational or positive internal energy.

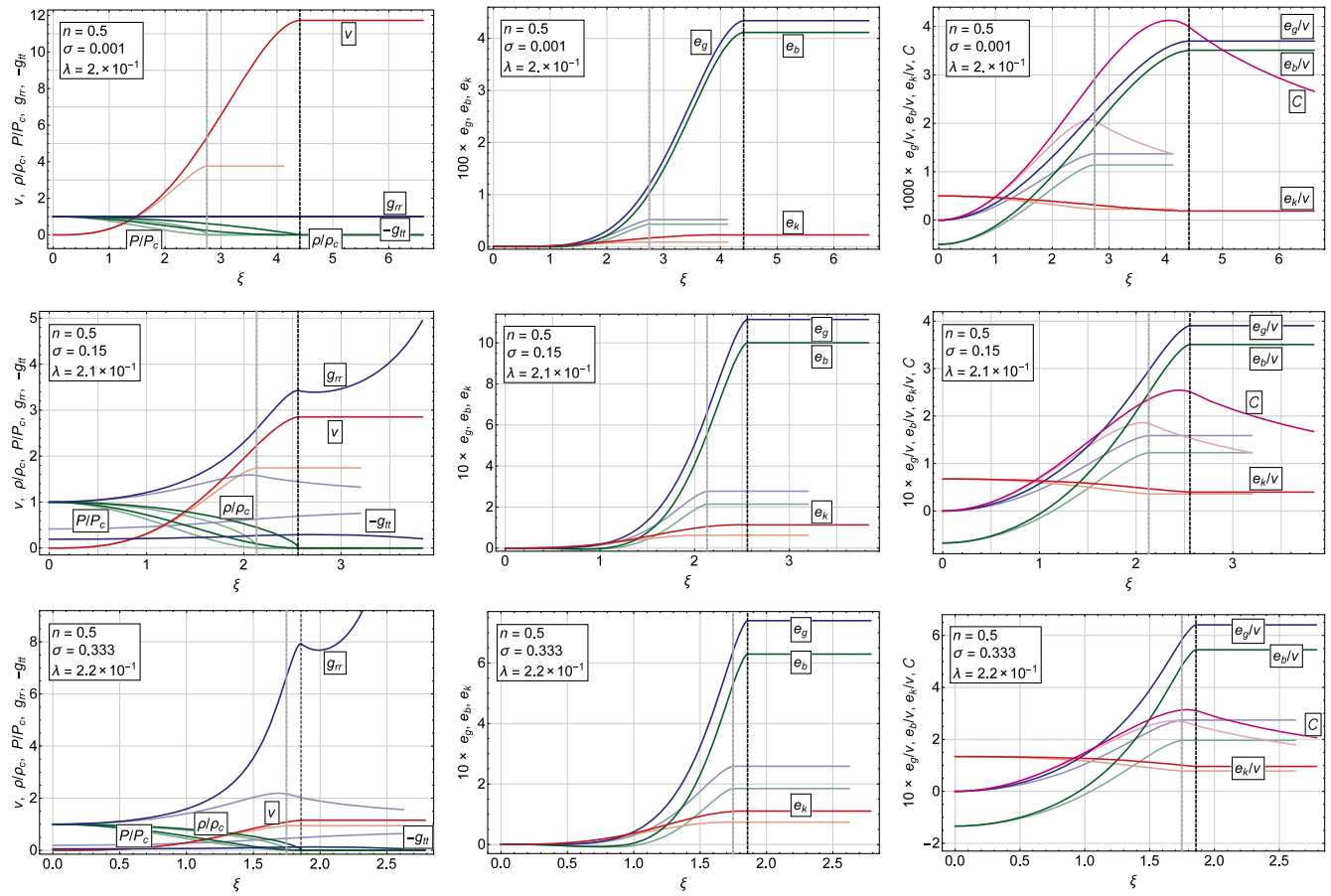

FIG. 13. Profile plots for polytropic index $n = 0.5$. *Left column:* Mass, density, pressure, and metric coefficients. *Middle column:* Gravitational, binding, and kinetic energy. *Right column:* Relative gravitational, binding, kinetic energy, and compactness.

The role of the cosmological constant in the behavior of the binding energy of the polytropes is represented in Fig. 11 for the same values of the polytrope index n and the dimensionless parameter λ as in the case of quantities ξ_1 and v_1. The binding energy function $\mathcal{B}_1(n;\sigma,\lambda)$ is always compared to the function $\mathcal{B}_1(n;\sigma,\lambda=0)$. In the case of $\lambda = 0$, there is $\mathcal{B}_1(n;\sigma=0) = 0$. For each of the $n = 1$, 1.5, 2, 2.5 polytropes, the binding energy σ profile reaches a maximum at some $\sigma < 0.1$ and then decreases to a minimum at the causality limit of the relativistic parameter σ. In the case of $n = 1$, 1.5 polytropes, the σ profile gives positive a dimensionless binding energy at the whole allowed range of σ. For the $n = 2$, 2.5 polytropes, there is a zero point of the binding energy σ profile, and behind this point, the binding energy is negative. On the other hand, for the polytropes with $n = 3$, 3.5, 4, the binding energy is negative for all the allowed values of σ, and the gravitational energy maintains the internal energy of the configuration. For the polytropes with $n = 3.5$, 4, having divergence of ξ_1 at the critical values of σ_f, the σ profiles of the binding energy are continuous at the critical points, but their derivative has a jump there. In the region of large values of σ, the binding energy decreases in the case of the $n = 4$ polytropes to the value $\mathcal{B}_1 \sim -0.27$ at the causality limit.

The influence of the cosmological constant parameter λ on the binding energy function $\mathcal{B}_1(n;\sigma,\lambda)$, demonstrated in Fig. 11, is concentrated to the cutoff in allowed values of the parameter σ for polytropes with fixed parameter n. We can also observe slight modifications of the σ profile of the binding energy function $\mathcal{B}_1(n;\sigma,\lambda)$, but modifications of the σ profiles that are large enough to be recognizable occur only for $\lambda \geq 10^{-3}$—increasing the parameter λ always increases the binding energy of the polytrope, if its other parameters are fixed.

For completeness, we present in Fig. 12 also the σ profiles of the relative binding energy related to the whole polytrope that is defined by $\mathcal{B}_1/v_1(n;\sigma,\lambda)$; again, the binding energy is related to the dimensionless gravitational mass of the polytrope. For $\lambda = 0$, there is $\mathcal{B}_1/v_1(n;\sigma=0) = 0$. We can see that the character of the σ profiles of $\mathcal{B}_1/v_1$ for the polytropes with $n = 1$, 1.5, 2, 2.5 is the same as for the binding energy, but their magnitude is larger since the gravitational mass parameter $v_1 < 1$. For the $n = 3$ polytropes, the σ profiles of the relative binding energy function $\mathcal{B}_1/v_1$ have a clear

minimum, while for the $n = 3.5$, 4 polytropes, they demonstrate jump to the zero point at the critical points of $\sigma_{\rm f}$ due to the behavior of mass parameter v_1. For the $n = 4$ polytropes, the relative binding energy is extremely small for $\sigma > \sigma_{\rm f2}$.

The influence of the cosmological constant parameter λ on the σ profiles of the relative binding energy function $\mathcal{B}_1/v_1(n;\sigma,\lambda)$ is illustrated in Fig. 12. Again, there is the cutoff in the allowed values of the parameter σ for polytropes with fixed parameter n, and very small modifications of the σ profiles relative to those with $\lambda = 0$ occur. They slightly grow with increasing λ, leading to a small increase of the relative binding energy $\mathcal{B}_1/v_1$.

IX. RADIAL PROFILES OF THE GRPS

Full understanding of the GRPs can be obtained by studying in detail the character of their internal spacetime structure represented by the metric coefficients and the distribution of the physical quantities in their interior, namely, the energy density; pressure; gravitational mass; and profiles of the compactness, gravitational, binding, and kinetic energy. The gravitational phenomena are properly characterized also by the embedding diagrams of the ordinary and the optical geometry of the central planes of the polytropes. In the spherically symmetric spacetimes, we have thus to find the radial profiles of the metric coefficients and the physical quantities mentioned above.

A. Construction of the profiles

We illustrate the detailed behavior of the polytropic spheres in dependence on the parameters n, σ, and λ, demonstrating in appropriately selected cases the radial profiles of the energy density, pressure, gravitational mass, and metric coefficients. These are completed by the embedding diagrams of the ordinary and optical geometry; by the radial profiles of the gravitational energy, binding energy, and the kinetic energy; and by the corresponding radial profiles of these energies related to the dimensionless mass parameter v_1 of the polytropes and the radial profiles of the compactness parameter. The results of the numerical calculations of the radial profiles are presented in series of figures. For fixed values of the parameters n and σ, the radial profiles are constructed for $\lambda = 0$ that are compared to radial profiles constructed for the appropriately chosen value of the cosmological parameter λ enabling clear demonstration of the role of the cosmological constant—naturally, for given values of the polytropic index n and the relativistic parameter σ, we choose the value of the cosmological parameter λ close to the critical cosmological parameter limiting the polytropes, $\lambda_{\rm crit}(n,\sigma)$, guaranteeing a clear illustration of the influence of the cosmological constant.

We construct the radial profiles in the case of four characteristic values of the polytropic index n, restricting thus the wide selection of the polytropic indexes used in constructing the global characteristics of the polytropes.

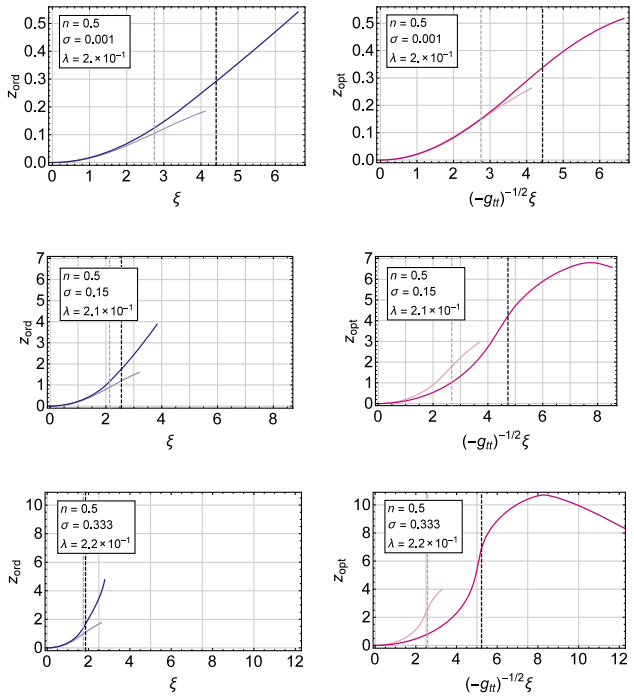

FIG. 14. Embedding diagrams for polytropic index $n = 0.5$. *Left column:* Ordinary geometry. *Right column:* Optical geometry.

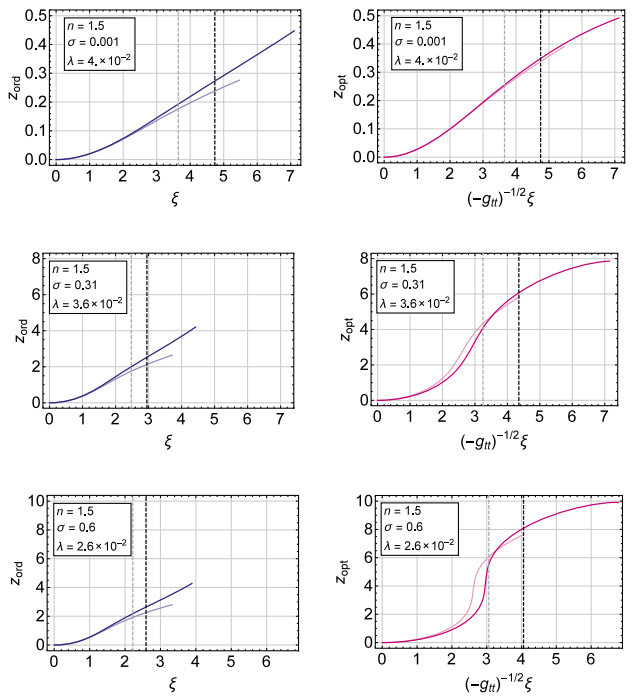

FIG. 15. Embedding diagrams for polytropic index $n = 1.5$. *Left column:* Ordinary geometry. *Right column:* Optical geometry.

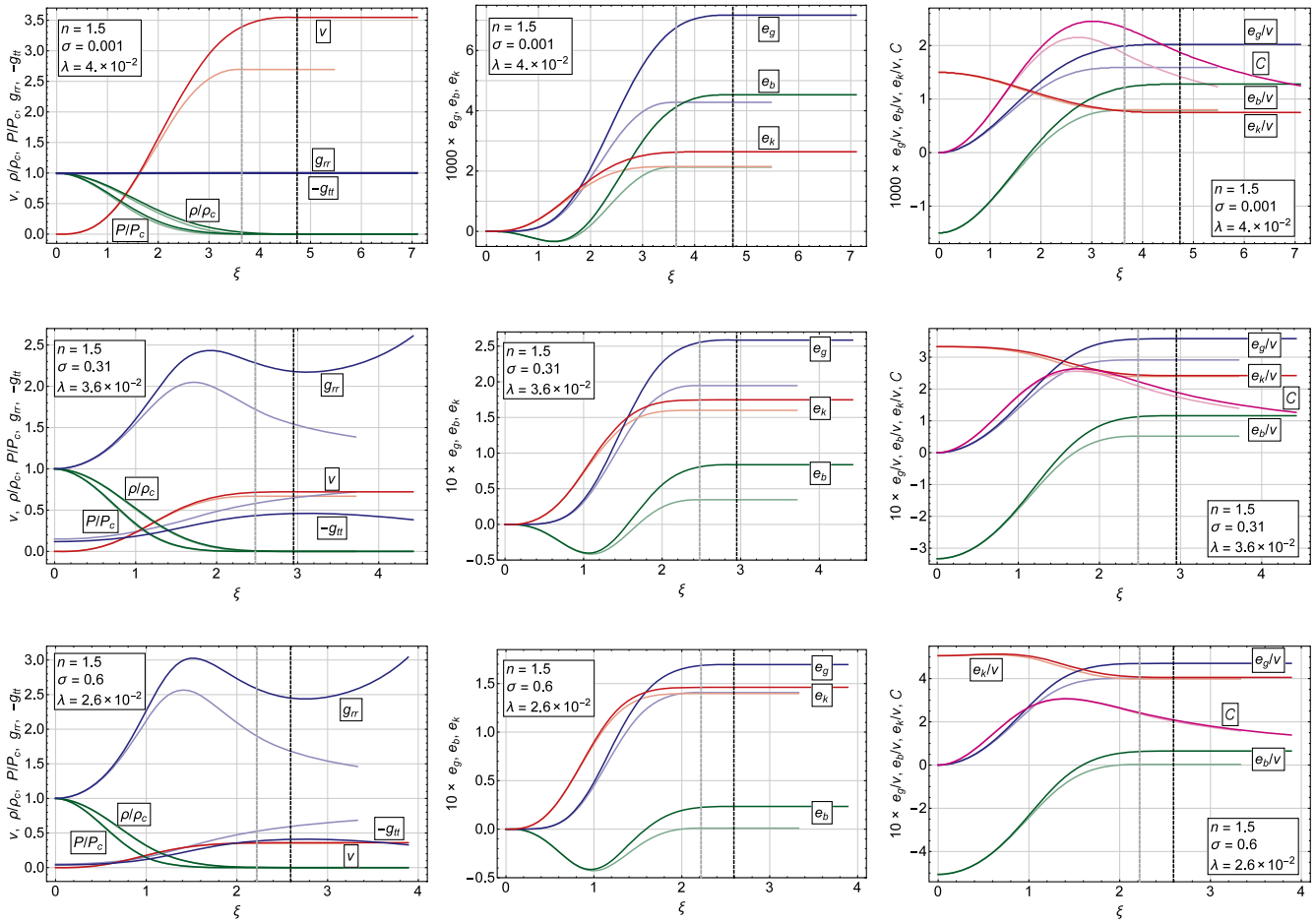

FIG. 16. Profile plots for polytropic index $n = 1.5$. *Left column:* Mass, density, pressure, and metric coefficients. *Middle column:* Gravitational, binding, and kinetic energy. *Right column:* Relative gravitational, binding, kinetic energy, and compactness.

We choose the most relevant polytropic indexes $n = 1.5$, 3 and the indexes $n = 0.5$, 3.5, enabling us to give a clear illustration of all the possible cases of the behavior of the GRPs. Note that the case of the $n = 1$ polytropes is similar to $n = 0.5$ polytropes, and the polytropes $n = 2$, 2.5 represent the transition of the $n = 1.5$ polytropes to the relativistic $n = 3$ polytropes. The $n = 4$ polytropes are similar to the case of $n = 3.5$ polytropes, but they are more extreme in the vicinity of the critical points of the relativistic parameter, $\sigma_{\rm f}$. The values of the parameter σ are selected from the whole allowed interval, up to the critical value determined by the causality limit. For all of the considered polytropic indexes n, we choose a very small relativistic parameter representing the nonrelativistic limit of the polytropes, $\sigma = 10^{-3}$, and the largest one representing the causal limit. We also select some intermediate value of σ in order to represent the characteristic intermediate polytropic configurations. We use one such σ for $n < 3$ but more such intermediate values of σ for $n = 3$ and $n = 3.5$ polytropes. For each value of the polytropic index n, we construct four sequences of radial profiles related to (a) the metric coefficients $-g_{tt}$, g_{rr}, energy density $\rho/\rho_{\rm c}$, pressure $p/p_{\rm c}$, and mass parameter v; (b) gravitational energy $e_{\rm g}$, binding energy $e_{\rm b}$, and kinetic energy $e_{\rm k}$; (c) relative gravitational energy $e_{\rm g}/v$, relative binding energy $e_{\rm b}/v$, relative kinetic energy $e_{\rm k}/v$, and compactness $\mathcal{C}$; and (d) embedding diagrams of the ordinary space $z_{\rm ord}$ and the optical space $z_{\rm opt}$.

All the radial profiles and the embedding diagrams are given for the polytropes with $n = 0.5$ in Figs. 13 and 14, respectively. The polytrope $n = 1.5$ case is reflected by Figs. 16 and 15, respectively. The case of $n = 3$ polytropes is illustrated in Figs. 18 and 17, respectively. The case of the $n = 3.5$ polytropes is represented in Figs. 19 and 20, respectively, where the profiles are given for the parameter σ chosen on both sides of the critical value of $\sigma_{\rm f}$.

B. Properties of the profiles

The dimensionless extension parameter ξ_1 increases with increasing polytropic index n and decreases with increasing relativistic parameter σ, while the mass parameter $v_1 = v(\xi_1)$ decreases with increasing polytropic index n and increasing parameter σ. Notice that in the polytropes

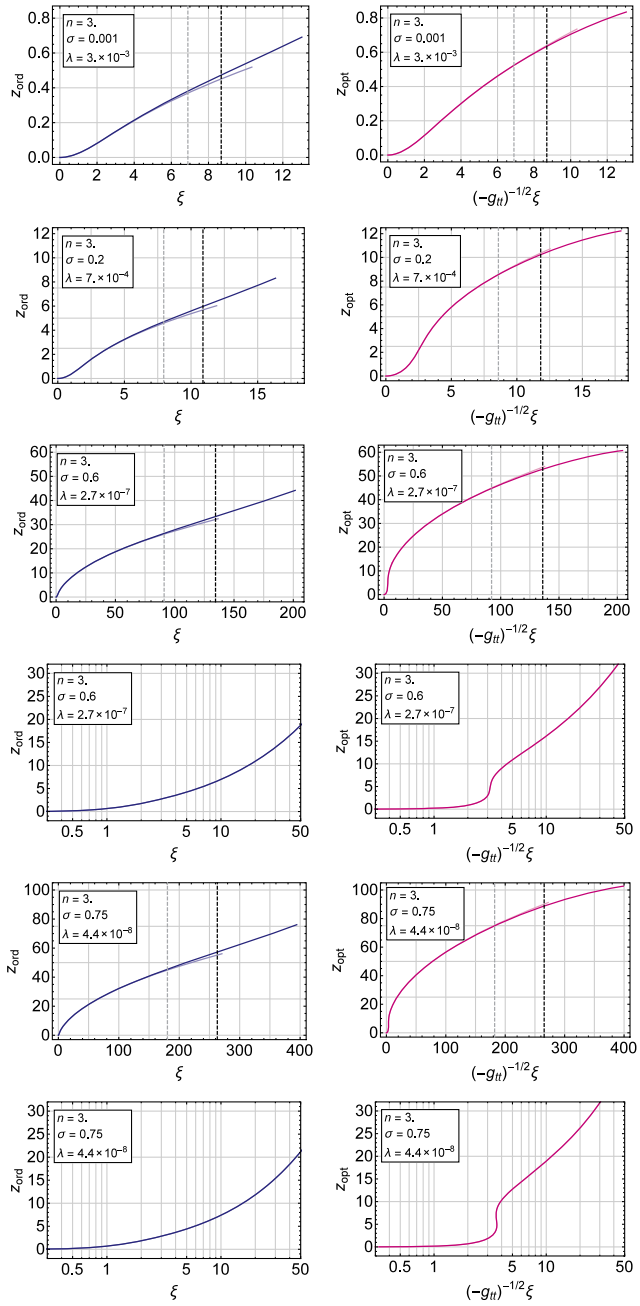

FIG. 17. Embedding diagrams for polytropic index $n = 3.0$. *Left column:* Ordinary geometry. *Right column:* Optical geometry. The S-shaped part in the third row plot is zoomed in the fourth row. The S-shaped part in the fifth row right plot is zoomed in the bottom row.

with large values of ξ_1 the density (and pressure) radial profiles are strongly decreasing near the origin $\xi = 0$, reaching values ~ 0 at $\xi \sim 2$ and decreasing exponentially slowly while approaching ξ_1. Similar behavior can be observed in such polytropes also for the mass parameter $v(\xi)$ that is nearly equal to its final value v_1 starting from $\xi \sim 2$. We can see that for the nonrelativistic or slightly relativistic polytropic configurations (having $\sigma < 0.2$) the dimensionless parameters determining the polytropic sphere, ξ_1 and v_1, are of the order of 1. For $n \leq 3$ polytropes with the relativistic parameter increasing, the mass parameter v_1 takes values smaller than 1, while the extension parameter ξ_1 increases substantially, exceeding 1, even by orders, for large values of the relativistic parameter, comparable to the value of causality limit. A special behavior is demonstrated by polytropes having high values of the polytropic index, e.g., $n = 3.5$, especially for values of σ close to the critical values of σ_f. Such configurations can have extremely large extension parameter ξ_1 and mass parameter $v_1 > 1$ even for large values of the relativistic parameter, $\sigma > \sigma_f$. Recall that at the critical values of the relativistic parameter, σ_f, static equilibrium polytropic configurations are not well defined for $\lambda = 0$, while any nonzero value of the cosmological parameter cuts out the polytropic configurations with $\sigma \sim \sigma_f$—see Fig. 3.

As can be intuitively expected, the metric coefficients are nearly constant, $g_{rr} \sim 1$ and $-g_{tt} \sim 1$, for very small values of the relativistic parameter, $\sigma < 0.01$, being slightly dependent on the polytropic index n; such spacetimes are nearly flat, demonstrating clearly that the relativistic parameter σ governs the intensity of the general relativistic effects in the polytropes. For $\sigma > 0.1$, the general relativistic effects described by the metric coefficients g_{rr} and g_{tt} become significant as the metric coefficients significantly vary inside the polytrope. Outside the polytropes with $\lambda \sim \lambda_{crit}$, the gravitational field varies strongly for small values of the polytropic index n and large enough parameter $\sigma > 0.1$, as the polytropes are compact enough while having their surface located near the static radius. For such polytropes, also, the radial profiles are strongly influenced by the cosmic repulsion (parameter λ), as demonstrated in Figs. 13–20. With the increasing polytropic index, the polytropes with $\lambda \sim \lambda_{crit}$ demonstrate suppression of the role of the cosmic repulsion in the character of the radial profiles. This suppression is evident especially in the case of the $n = 3.5$ polytropes with $\sigma > \sigma_f$ having large extension parameter ξ_1 and $v_1 > 1$.

The magnitude of the gravitational binding energy is positive everywhere in the polytrope, similarly to the kinetic energy of the polytrope. The binding energy is negative in the central parts of the polytrope and becomes positive in the outer region of the polytrope for the whole allowed interval of σ, if $n = 0.5$, 1.5. However, such a behavior occurs in the polytropes with $n = 3$ only for appropriately low values of σ—the binding energy is negative at all radii of such polytropes for a large enough relativistic parameter. The critical value of σ for altering the mixed to fully negative radial profile of the binding energy strongly decreases with increasing n, being $\sim 10^{-2}$ for $n = 3$. Of course, the same properties are valid for the gravitational, kinetic, and binding energy related to the dimensionless gravitational mass v of the polytropes.

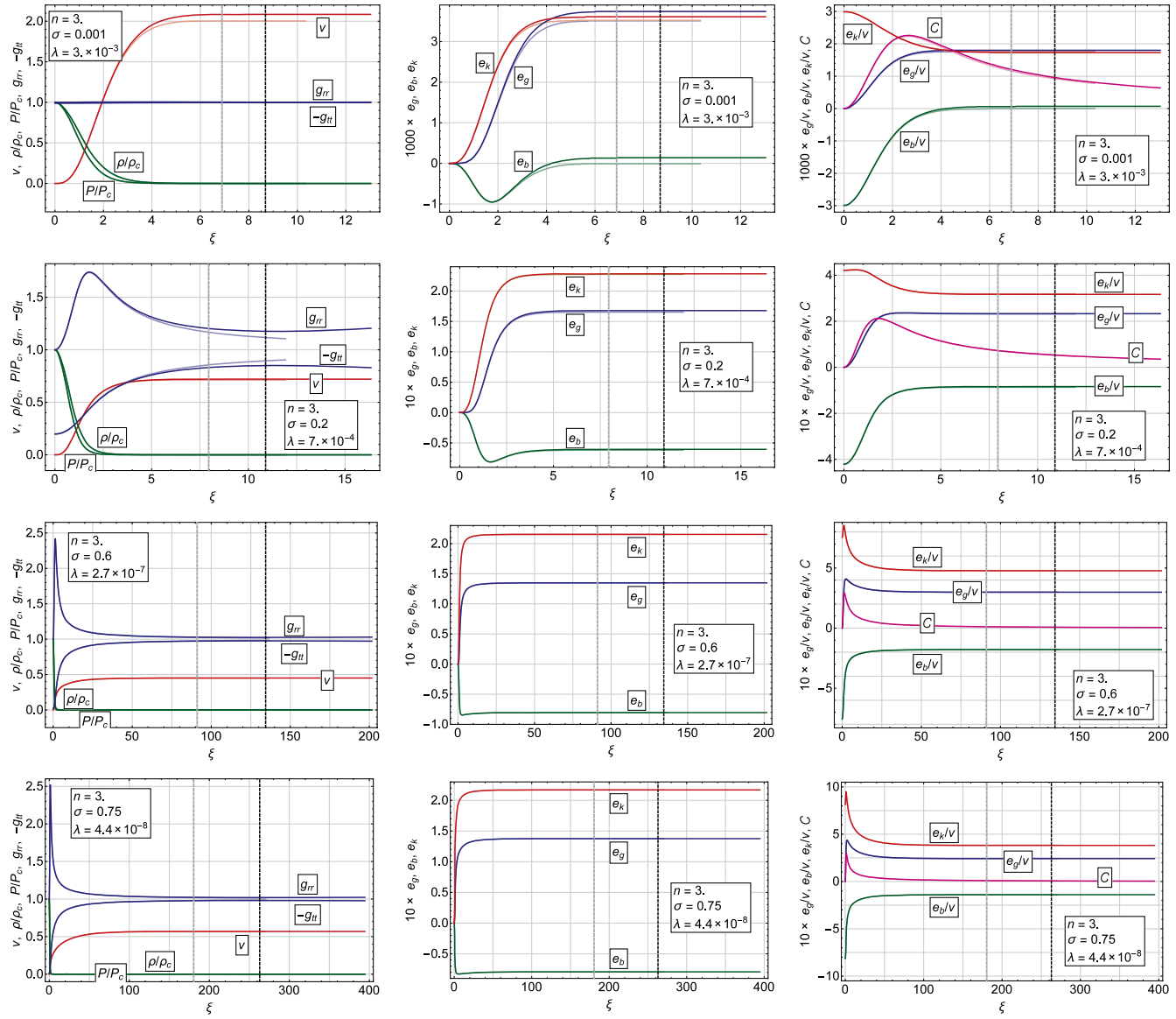

FIG. 18. Profile plots for polytropic index $n = 3.0$. *Left column:* Mass, density, pressure, and metric coefficients. *Middle column:* Gravitational, binding, and kinetic energy. *Right column:* Relative gravitational, binding, kinetic energy, and compactness.

The embedding diagrams of the ordinary projected space give an illustration of the curvature of the space inside the polytrope. We can clearly see that the curvature of the ordinary space increases slightly with increasing polytropic index n, but it increases very strongly with the relativistic parameter σ increasing while n is fixed. The embedding diagrams of the optical space can be extremely useful for understanding the properties of the polytropes related to the possibility of the existence of extremely curved regions containing trapped null geodesics. The existence of such regions is indicated by the radial profile of the optical space demonstrating two turning points that could occur even deeply inside the polytrope, although no effect of this kind has to be related to the external characteristics of the polytrope, determined by its dimensionless radius ξ_1 and dimensionless mass v_1. Clearly, such extremely curved regions can occur only in the highly relativistic spacetimes with sufficiently high values of the relativistic parameter σ related to the polytropes with high values of the polytropic index, $n \geq 2$. For such GRPs with extremely curved regions, the global compactness factor does not demonstrate the extremal compactness since such GRPs have largely extended low-density regions near their surfaces. Technically, this means that $\xi_1 \gg 1$ and $v(\xi_1) \sim 1$ so that the global compactness drops down to $\mathcal{C} \ll 1/3$.

Concerning the effects of the cosmological constant, they can be clearly important only in the extremely low-density polytropic configurations, having very small central density and high enough cosmological parameter λ. We can state that, quite generally, the influence of the cosmological

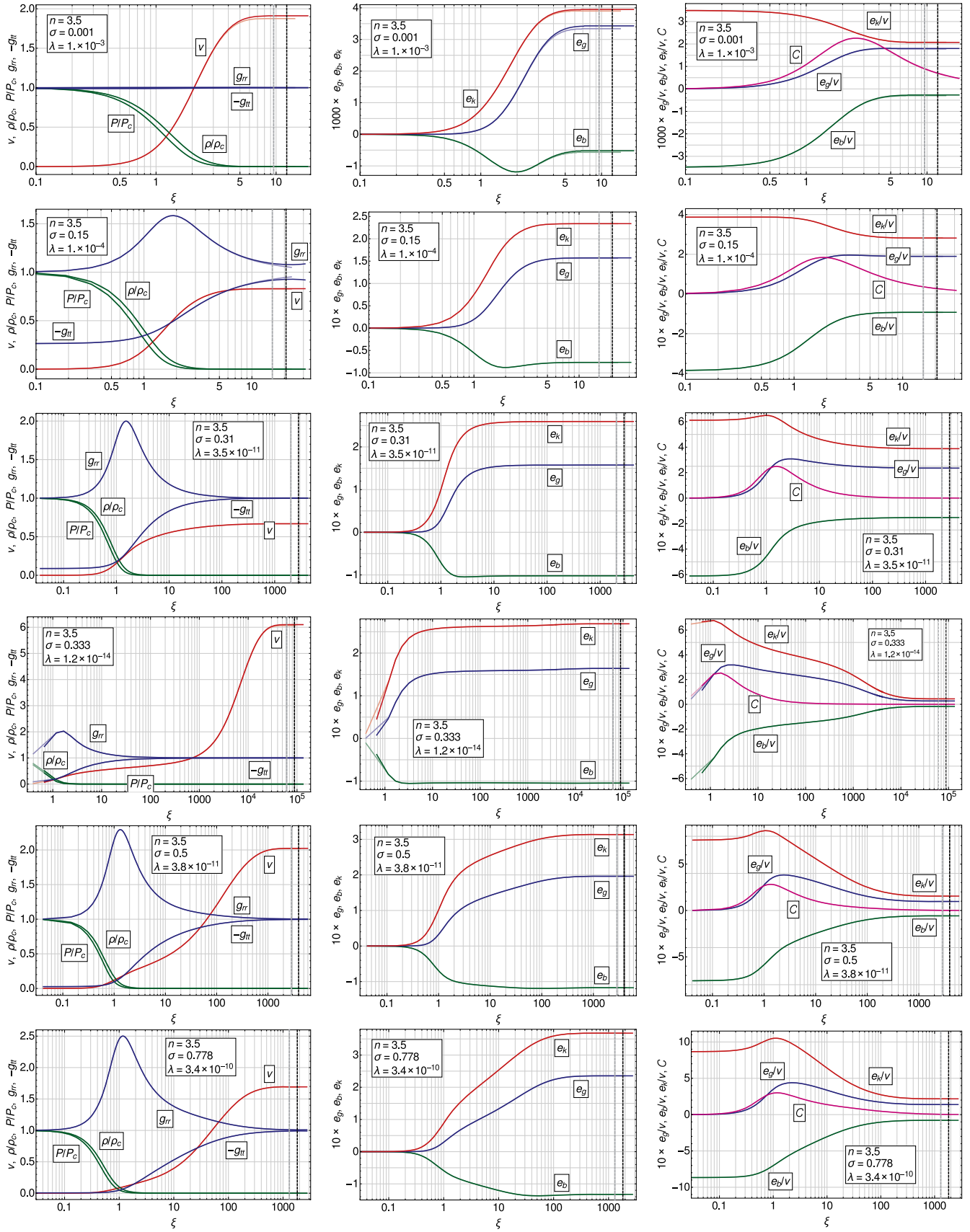

FIG. 19. Profile plots for polytropic index $n = 3.5$. *Left column:* Mass, density, pressure, and metric coefficients. *Middle column:* Gravitational, binding, and kinetic energy. *Right column:* Relative gravitational, binding, kinetic energy, and compactness.

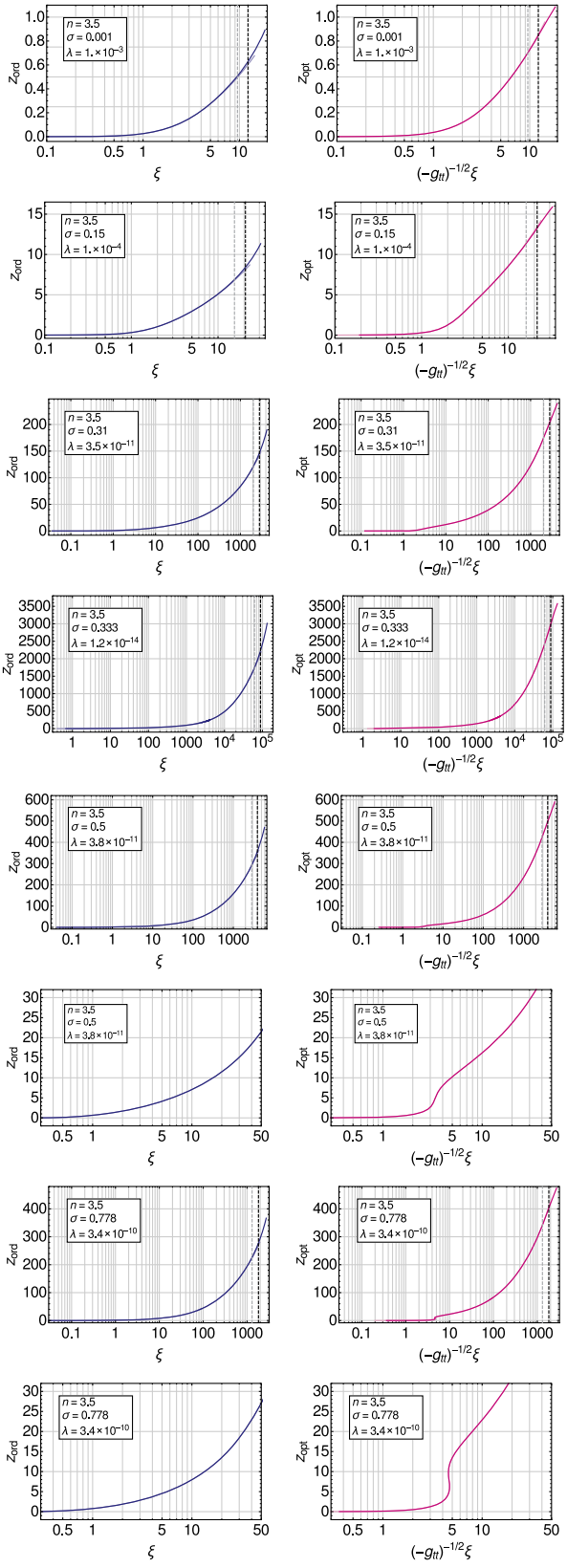

FIG. 20. Embedding diagrams for polytropic index $n = 3.5$. *Left column:* Ordinary geometry. *Right column:* Optical geometry. The S-shaped parts in fifth and seventh rows are repeated in zoomed form in sixth and eighth rows, respectively.

constant always increases the values of the extension and mass parameters of the polytrope, its metric coefficients, or the magnitude of the gravitational energy. The influence of the cosmic repulsion on the structure of polytropic configurations with the index $n \leq 3$ can be relevant for relatively large values of $\lambda > 10^{-7}$ when some observable effects could be expected, especially in the low-density polytrope configurations; we have convinced ourselves that the influence of the cosmological parameter is negligible for $\lambda < 10^{-7}$. Such GRPs could be relevant and applicable for very massive and very extended objects with very low density. The influence of the cosmological constant on the extension, mass, and the radial profiles can be very large for the polytropes with low values of the polytropic index, especially for $n = 0.5$. On the other hand, for the polytropes with $n = 3$, 3.5, the influence of the cosmological constant is strong in the case of their extension, but it is small in the case of the mass parameter and the radial profiles of all quantities for polytropes with very small values of σ, and it is even negligible for $\sigma > 0.1$.

It is quite natural to consider the possibility to model dark matter halos as polytropic spheres with $n = 0.5$ or $n = 1.5$ and test the role of the repulsive cosmological constant in situations when $\lambda \sim \lambda_{\rm crit}$. The large enough cosmological parameter significantly restricts the polytropes in dependence on the relativistic parameter σ. In the case of the polytropes with index $n = 3$, 3.5, the situation is more complex, as these polytropes are influenced in their extension by any $\lambda > 0$ in the vicinity of the critical values of the relativistic parameter $\sigma_{\rm f}$. Moreover, for values of λ large enough, the existence of the polytropes is forbidden—the $n = 4$ polytropes cannot exist for $\lambda > 10^{-3}$. Further, we can conclude that the cosmological constant is irrelevant for very dense polytropes with high central densities and extremely small cosmological parameters, except the effect of restricting the extension of the polytropes with the relativistic parameter $\sigma \sim \sigma_{\rm f}$.

X. POLYTROPE RADIUS MODIFIED BY THE COSMIC REPULSION

To illustrate clearly the role of the cosmological constant (vacuum energy) in the character of the GRPs, it is instructive to relate the extension of the polytropic spheres to the so-called static radius of their external spacetime [15]. The static radius is determined by the formula [31,95]

$$r_{\rm s} = \left(\frac{3r_{\rm g}}{2\Lambda}\right)^{1/3}. \tag{133}$$

At the static radius, the gravitational attraction of the central mass source (i.e., the galaxy and its halo) is just balanced by the cosmic repulsion. The static radius defines the region of gravitational binding [31], and it should be stressed that the region of strong cosmological-constant repulsion effects starts behind the static radius where the cosmic

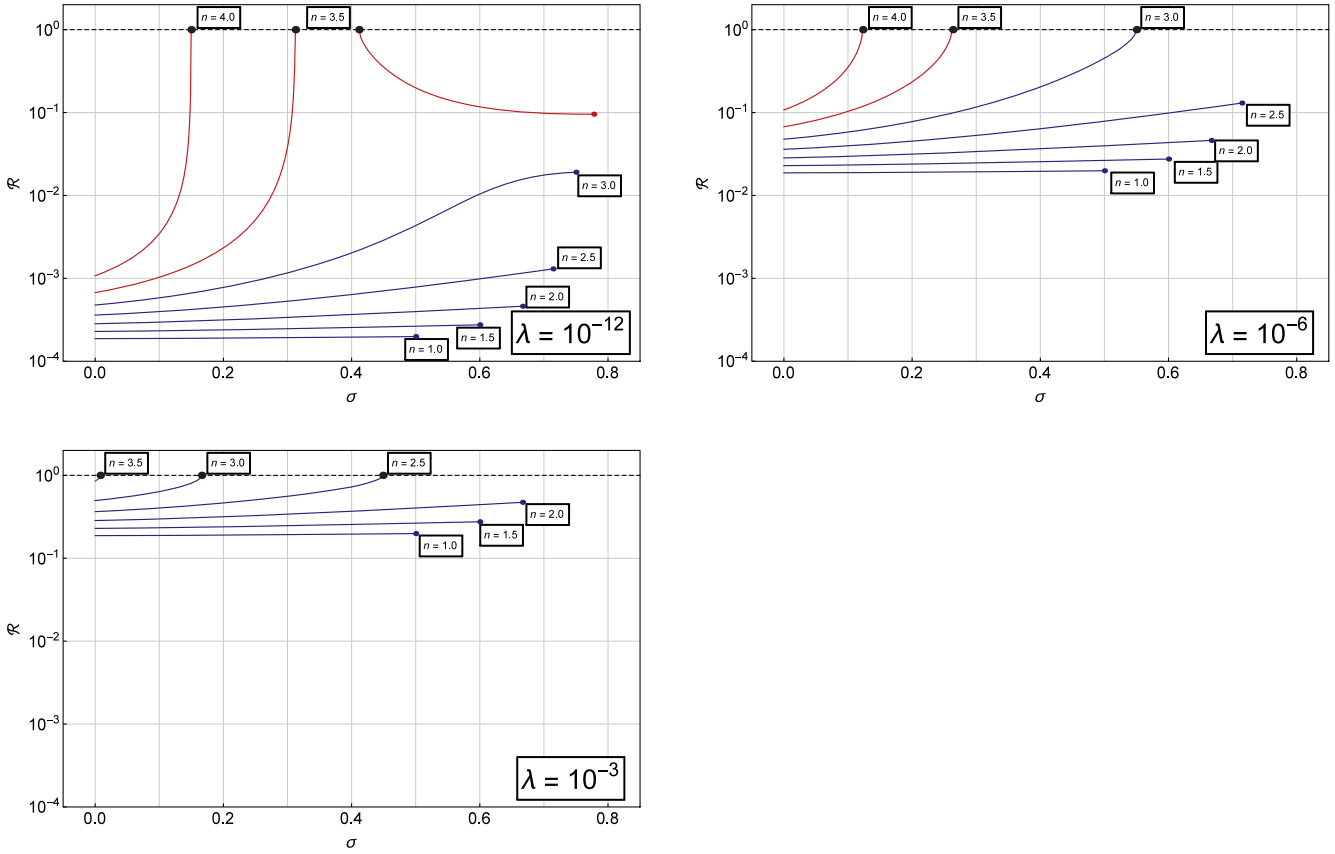

FIG. 21. The results of numerical computations of the configuration-to-static radius ratio $\mathcal{R}$ for $\lambda = 10^{-12}$ (top left), $\lambda = 10^{-6}$ (top right), and $\lambda = 10^{-3}$ (left) with polytropic index n ranging from 1.0 to 4.0 with steps of 0.5. While the positions of the small terminating points stem from the restriction on the sound speed at the configuration center, the larger black terminating points located at $\mathcal{R} = 1$ express the fact that the configuration radius cannot be extended behind the static radius. With λ increasing, the curves for higher n gradually vanish.

repulsive acceleration maintains the gravitational attraction and the cosmic expansion occurs [29,95,142,143]. Using the quantities characterizing the spherical polytropes, we can express the static radius of the external spacetime of the polytropes in the form

$$r_s = \frac{3v(\xi_1)^{1/3}}{2\lambda}\left[\frac{\sigma(n+1)c^2}{4\pi G\rho_c}\right]^{1/2} = \mathcal{L}\frac{3v(\xi_1)^{1/3}}{2\lambda}. \quad (134)$$

Then, we can introduce a dimensionless "cosmologically" modified radius, i.e., the radius expressed in units of the static radius

$$\mathcal{R} = \frac{R}{r_s} = \frac{\xi_1(2\lambda)^{1/3}}{[3v(\xi_1)]^{1/3}} \quad (135)$$

reflecting the role of the cosmic repulsion in the character of the general relativistic polytropic spheres. It is clear that this role is growing with the cosmologically modified radius increasing, but the modified radius does not depend on the central density ρ_c explicitly but only implicitly due to magnitude of the cosmological parameter. We can see immediately that the cosmological parameter λ is the most relevant one; however, for relatively large values of the polytropic index ($n \geq 3$) and the relativistic parameter ($\sigma > 0.6$), the dimensionless radius ξ_1 can grow substantially. The results of the numerical calculations are given in Fig. 21. The limits on the dimensionless radius of the polytrope expressed in units of the static radius of the external spacetime are given in terms of the functions $\mathcal{R}(\sigma, n, \lambda)$ considered for the characteristic values of the cosmological parameter λ and the polytropic index n that were used for the deduction of GRP global characteristics. The restrictions have the upper limit at the ratio $\mathcal{R} = 1$ and become stronger with the increasing value of λ and increasing value of n. For $\lambda = 10^{-12}$, the upper limit of $\mathcal{R} = 1$ is relevant for polytropes with $n = 3.5, 4$ from the considered values of n, for $\lambda = 10^{-6}$, and also the $n = 3$ polytropes can reach the upper limit of $\mathcal{R} = 1$, while for $\lambda = 10^{-3}$, the polytrope $n = 2.5$ reaches the limit of $\mathcal{R} = 1$, too, but the polytropes with $n = 4$ are completely forbidden for such a high value of λ. Of course, the range of allowed values of the relativistic parameter σ for a polytrope with fixed index n decreases with increasing parameter λ.

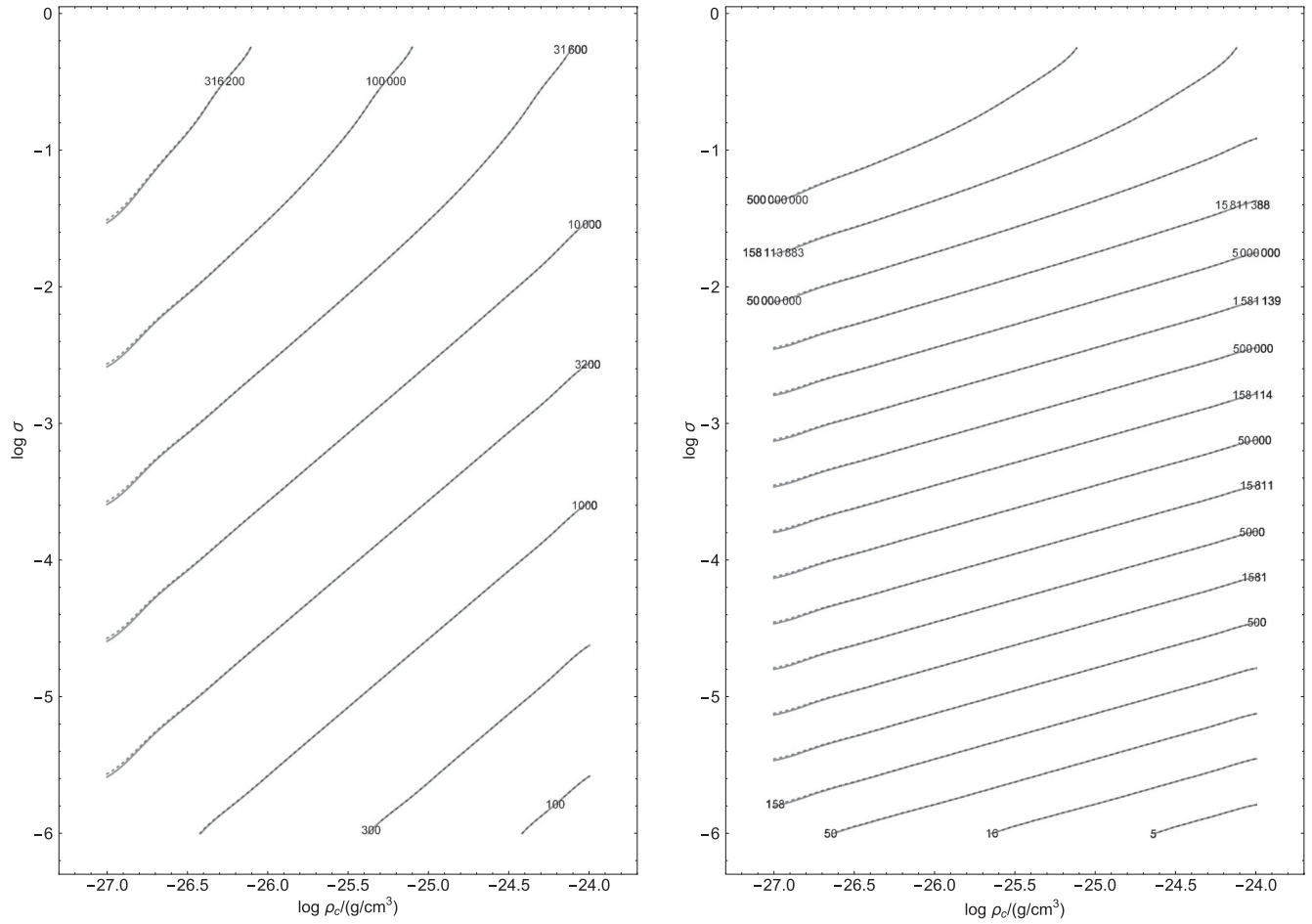

FIG. 22. Comparison of contours $R = \text{const}$ (R in kpc, left) and $M = \text{const}$ (M in $10^{12}\mathrm{M}_{\odot}$, right) related to the observationally established cosmological constant (solid) and vanishing cosmological constant (dashed) in the parameter space $\sigma - \rho_{\mathrm{c}}$ for polytropes with $n = 1.5$. The presence of cosmological constant increases the radius up to a percent and mass up to a few percent for a fixed σ and ρ_{c}, particularly for small central densities ρ_{c}.

In the special case of uniform energy density spheres (GRPs with the polytropic index $n = 0$), the cosmologically modified dimensionless radius reads

$$\mathcal{R} = (2\lambda)^{1/3}. \tag{136}$$

For the $n = 0$ GRPs, the vacuum energy parameter must satisfy the condition $\lambda < 1/2$—we see immediately that extension of the $n = 0$ polytropes cannot exceed the static radius of the external spacetime. The same statement holds for GRPs with any value of the polytropic index n as demonstrated by numerical calculations presented above. We have to stress that increasing the value of the vacuum energy parameter λ means decreasing central density of the polytrope, if the vacuum energy is assumed to be fixed by the cosmological tests.

The analysis demonstrates that extension of the low-density polytropes strongly increases with decreasing central density related to the cosmic repulsion by the cosmological parameter λ. The rate of the polytropic extension decrease depends strongly on the polytropic index n and the relativistic parameter σ. We can observe in Fig. 4 that there can even be two branches of the polytropes with fixed polytropic index $n > 3$.

We can summarize that the results of the numerical analysis of the extension of the low-density polytropic spheres, where the role of the cosmological parameter λ is relevant, imply that extension of the GRPs cannot exceed the static radius of their external spacetime. This is a demonstration of the fact that the gravitationally bound systems are limited by the static radius, indicated for the first time in Ref. [31].

The cosmologically modified polytrope radius is the most representative quantity when we relate the polytropes to the most extended objects on the cosmic scales. On the other hand, in the opposite extreme, related to the most compact objects, we have to use as the proper measure the dimensionless radius related to the gravitational radius of the object, given by

$$\mathcal{R}_{\mathrm{g}} = \frac{R}{r_{\mathrm{g}}} = \mathcal{C}^{-1}. \tag{137}$$

For very compact objects with large central energy, the role of the cosmological constant is quite negligible because the cosmological parameter λ has to be extremely low.

XI. MODELS OF GALACTIC HALO

Finally, we present some comments on the possibility to model galactic dark matter halos by the GRPs. For these purposes, it is useful to express the length and mass scales of the relativistic polytropes in the form adjusted to the astrophysically relevant, galactic conditions. Therefore, we express the length scales (132) in the form

$$\mathcal{L} = 1.06\frac{[\sigma(n+1)]^{1/2}}{\rho_{\rm c}^{1/2}}(100\ {\rm kpc}), \tag{138}$$

$$\mathcal{M} = 2.22\frac{[\sigma(n+1)]^{3/2}}{\rho_{\rm c}^{1/2}}(10^{18}\,{\rm M}_{\odot}), \tag{139}$$

with $\rho_{\rm c}$ to be substituted in units of $10^{-20}\ {\rm g/cm^3}$. The length scale of galactic halos related to typical galaxies, similar to the Milky Way galaxy, is estimated to be 100–200 kpc, while the estimated mass of the halo is considered to be about $(1\text{–}5)\times 10^{12}\,{\rm M}_{\odot}$. Of course, in the case of extremely large and massive galaxies and galaxy clusters, the extension of the halo can be up to 1 Mpc, and the halo mass could be as large as $10^{15}\,{\rm M}_{\odot}$ [144].

The polytropic spheres with given mass and length scales are determined by the solution of the structure equations given by the radial coordinate $\xi_1(n,\sigma,\lambda)$ and the related mass parameter $v_1(n,\sigma,\lambda)$. Generally, the exact solutions can strongly modify the length and mass scales; however, for low values of the parameter n and nonrelativistic dark matter with $\sigma \ll 1$, the length and mass scales are decisive. Then, we can obtain the GRP extension and mass in agreement with the galactic halo estimates for $\sigma(n+1) < 10^{-4}$. However, the central density of such polytropes has to be very small.

Detailed analysis of the possible matching of the GRP extension and mass to the CDM halo extension and mass is planned for a future paper. Here, using the numerical methods, we give insight into the role of the observationally given cosmological constant on the fitting of the length and mass of the polytropes to the astrophysically relevant values for a concrete polytrope model with parameter $n = 3/2$ corresponding to the nonrelativistic gas. In Fig. 22, the constant values of the polytrope extension R (and mass M) are given as the functions of the parameters σ and $\rho_{\rm c}$ that give also the parameter λ. The contours related to the cosmological constant with the observationally given value of $\Lambda \sim 10^{-56}\ {\rm cm^{-2}}$ are related to those corresponding to $\Lambda = 0$. For the $n = 3/2$ polytropes, the influence of the cosmological constant is strongest for small values of σ, being on the level of 1% for the extension and 3% for the mass of the polytrope.

XII. CONCLUDING REMARKS

We have constructed fully general relativistic models of polytropic spheres immersed in the spacetime with the relict repulsive cosmological constant $\Lambda = 1.3\times 10^{-56}\ {\rm cm^{-2}}$, indicated by wide variety of recent cosmological tests. The polytropic spheres are characterized by three dimensionless parameters, namely, by the polytropic index n, the relativistic parameter $\sigma = p_{\rm c}/\rho_{\rm c}$ reflecting the role of the (special) relativistic effects in their structure, and the cosmological parameter $\lambda = \rho_{\rm vac}/\rho_{\rm c}$ reflecting the role of the vacuum energy density (the repulsive cosmological constant) in their structure. We have demonstrated that in dependence on the polytropic index n, and the relativistic parameter σ, the GRPs are not allowed for the values of the cosmological parameter $\lambda > \lambda_{\rm crit}(n,\sigma)$. The value of $\lambda_{\rm crit}$ increases with the polytropic index increasing and the relativistic parameter decreasing for the index $n \leq 3$, while it exhibits more complex behavior for $n = 3.5$, 4, when it can grow with increasing σ. There exist even some singular states for $n > 3.34$ polytropes, when the solutions are not allowed for special values of the relativistic parameter [141]. For example, we have found that the $n = 3.5$ polytropes are forbidden for one specific value of $\sigma_{\rm f} = 0.314$, while for the $n = 4$ polytropes, there are two forbidden values of the relativistic parameter $\sigma_{\rm f1} = 0.1503$, $\sigma_{\rm f2} = 0.338$. For these special values of σ, the extension of the polytropes diverges. However, the cosmological constant naturally cutoffs these divergent radii, as the radius of the polytropic configurations cannot exceed the static radius of the external spacetime, determined by the combined effect of the cosmological constant and the mass of the polytrope.

The length and mass scales of the GRPs with fixed polytropic index n are characterized by the central density $\rho_{\rm c}$ and the relativistic parameter σ. Both of them grow with the central density decreasing and the relativistic parameter increasing. The real extension of the polytropic spheres is influenced by the cosmological parameter λ, if it is high enough (and the central density is low enough, allowing for sufficiently high values of λ).

Since the dependence of mass and length scales on the central density $\rho_{\rm c}$ is of the same character, while it has inverse character in the case of the relativistic parameter σ, we can find, for any value of the polytropic index n, the parameters $\rho_{\rm c}$ and σ determining a polytropic sphere with prescribed values of the radius R and mass M. Of course, it can be done in the region of allowed values of the cosmological parameter λ.

Adjusting properly the central density of the polytrope, we are able to simulate properties of astrophysical objects in a wide range, starting in the region of extremely compact (neutron or strange) stars for extremely high central densities, through the standard stars and stellar clusters and finishing in the region of extremely extended low-density polytropic

structures that could represent large cold dark matter halos. We demonstrate that both the extension and mass of the most extended polytropic spheres, when the role of the cosmological constant has to be very important, putting even strong limits on the extension of such structures, can be in agreement with the data restricting dark matter halos—their extension and mass have to be ~ 100 kpc and $\sim 10^{12}\,M_\odot$ for galaxies of the type of the Milky Way, going up to ~ 1 Mpc and $\sim 10^{14}\,M_\odot$ for the largest galaxies [145] or even larger radius and mass for galaxy clusters. It is interesting that the polytropic spheres can be relevant also in the framework of the so-called little inflation [146] related to the first-order phase transition of quark-gluon plasma to the hadron phase at non-negligible baryon number [147] that implies the existence of dark matter halos of mass $M_{\rm cluster} \sim 10^6 M_\odot$ relevant for the physics of globular clusters and emergence of the first stars [148].

We have demonstrated that the extension of the GRPs cannot exceed the so-called static radius of their external spacetimes. Such a result supports idea of the static radius (or turnaround radius) representing an extension limit on gravitationally bounded configurations in the expanding universe governed by the cosmological constant [15,31,95].

In objects with a central density large enough, representing all the cases of compact objects, stars, and star clusters, the role of the repulsive cosmological constant is clearly quite negligible, since the cosmological parameter λ is extremely small in such situations due to high central densities. On the other hand, the numerical analysis shows that the relict repulsive cosmological constant has a relevant influence on the structure of GRPs when the length scale $\mathcal{L}$ becomes comparable with the cosmological length scale $\sim\Lambda^{-1/3}$. It is clear that $\mathcal{L}$ increases with σ increasing and ρ_c decreasing, and thus we can expect a strong role of Λ in very low-density polytropic configurations. The influence of the relict cosmological constant can be also amplified for polytropes with the polytropic index high enough. For example, in the case of $n > 3.5$, the influence of $\lambda > 0$ can lead to an instability of static polytropic configurations found in the case of $\lambda = 0$.

The stability of the general relativistic polytropic spheres has been shortly discussed in Ref. [149]. In the case of uniform density spheres, detailed discussion can be found also in Ref. [150]. We shall discuss the stability of the polytropes in detail in a future paper.

We also plan to study the influence of the repulsive cosmological constant on the so-called adiabatic fluid spheres, generalizing thus the results of Ref. [151], where the equation of state is considered in the more "popular" form that can be directly related to the perfect-gas equation of state, $p = K\rho_g^\gamma$, with ρ_g being the rest-mass density of gas and γ being the adiabatic index. We can expect that for the nonrelativistic gas, when $\rho \sim \rho_g$, the adiabatic spheres will be of similar character as the GRPs considered in the present paper, but significant differences occur for relativistic gas. The adiabatic spheres are governed by two structure equations with three parameters of the same meaning as those related to the polytropic spheres. However, the adiabatic structure equations are more complex in comparison to the polytrope structure equations; e.g., they do not alow for the existence of special solutions determined by elementary functions, as is the case of the $n = 0$ polytropes.

ACKNOWLEDGMENTS

The authors acknowledge the Institutional support of the Silesian University. One of the authors (Z. S.) acknowledges the Albert Einstein Center for Gravitation and Astrophysics supported by the Czech Science Foundation Grant No. 14-37086G. Authors J. N. and Z. S. thank the Silesian University Grant No. SGS/14/2016.

[1] A. D. Linde, *Particle Physics and Inflationary Cosmology* (Gordon and Breach, New York, 1990).
[2] L. M. Krauss and M. S. Turner, Gen. Relativ. Gravit. **27**, 1137 (1995).
[3] J. P. Ostriker and P. J. Steinhardt, Nature (London) **377**, 600 (1995).
[4] L. M. Krauss, Astrophys. J. **501**, 461 (1998).
[5] N. Bahcall, J. P. Ostriker, S. Perlmutter, and P. J. Steinhardt, Science **284**, 1481 (1999).
[6] R. R. Caldwell, R. Dave, and P. J. Steinhardt, Phys. Rev. Lett. **80**, 1582 (1998).
[7] C. Armendariz-Picon, V. Mukhanov, and P. J. Steinhardt, Phys. Rev. Lett. **85**, 4438 (2000).
[8] L. Wang, R. R. Caldwell, J. P. Ostriker, and P. J. Steinhardt, Astrophys. J. **530**, 17 (2000).
[9] D. N. Spergel *et al.*, Astrophys. J. Suppl. Ser. **170**, 377 (2007).
[10] A. G. Riess *et al.*, Astrophys. J. **123**, 145 (2004).
[11] R. Caldwell and M. Kamionkowski, Nature (London) **458**, 587 (2009).
[12] C. Adami, F. Durret, L. Guennou, and C. Da Rocha, Astron. Astrophys. **551**, A20 (2013).
[13] P. A. R. Ade *et al.* (Planck Collaboration), Astron. Astrophys. **571**, A12 (2014).
[14] C. W. Misner, K. S. Thorne, and J. A. Wheeler, *Gravitation* (Freeman, San Francisco, 1973).

[15] Z. Stuchlík, Bull. Astron. Inst. Czech. **34**, 129 (1983).
[16] Z. Stuchlík, Bull. Astron. Inst. Czech. **35**, 205 (1984).
[17] J.-P. Uzan, G. F. R. Ellis, and J. Larena, Gen. Relativ. Gravit. **43**, 191 (2011).
[18] C. Grenon and K. Lake, Phys. Rev. D **81**, 023501 (2010).
[19] P. Fleury, H. Dupuy, and J.-P. Uzan, Phys. Rev. D **87**, 123526 (2013).
[20] J. T. Firouzjaee and T. Feghhi, arXiv:1608.05491.
[21] G. C. McVittie, Mon. Not. R. Astron. Soc. **93**, 325 (1933).
[22] B. C. Nolan, Phys. Rev. D **58**, 064006 (1998).
[23] R. Nandra, A. N. Lasenby, and M. P. Hobson, Mon. Not. R. Astron. Soc. **422**, 2945 (2012).
[24] R. Nandra, A. N. Lasenby, and M. P. Hobson, Mon. Not. R. Astron. Soc. **422**, 2931 (2012).
[25] N. Kaloper, M. Kleban, and D. Martin, Phys. Rev. D **81**, 104044 (2010).
[26] K. Lake and M. Abdelqader, Phys. Rev. D **84**, 044045 (2011).
[27] A. M. da Silva, M. Fontanini, and D. C. Guariento, Phys. Rev. D **87**, 064030 (2013).
[28] B. C. Nolan, Classical Quantum Gravity **31**, 235008 (2014).
[29] Z. Stuchlík, Mod. Phys. Lett. A **20**, 561 (2005).
[30] F. Kottler, Ann. Phys. (Berlin) **56**, 401 (1918).
[31] Z. Stuchlík and S. Hledík, Phys. Rev. D **60**, 044006 (1999).
[32] Z. Stuchlík, Acta Phys. Slovaca **50**, 219 (2000).
[33] C. G. Böhmer, Gen. Relativ. Gravit. **36**, 1039 (2004).
[34] B. Carter, in *Black Holes*, edited by C. D. Witt and B. S. D. Witt (Gordon and Breach, New York, 1973) p. 57.
[35] Z. Stuchlík, Bull. Astron. Inst. Czech. **41**, 341 (1990).
[36] Z. Stuchlík and M. Calvani, Gen. Relativ. Gravit. **23**, 507 (1991).
[37] Z. Stuchlík and S. Hledík, Classical Quantum Gravity **17**, 4541 (2000).
[38] K. Lake, Phys. Rev. D **65**, 087301 (2002).
[39] P. Bakala, P. Čermák, S. Hledík, Z. Stuchlík, and K. Truparová, Central Eur. J. Phys. **5**, 599 (2007).
[40] M. Sereno, Phys. Rev. D **77**, 043004 (2008).
[41] T. Müller, Gen. Relativ. Gravit. **40**, 2185 (2008).
[42] T. Schücker and N. Zaimen, Astron. Astrophys. **484**, 103 (2008).
[43] J. R. Villanueva, J. Saavedra, M. Olivares, and N. Cruz, Astrophys. Space Sci. **344**, 437 (2013).
[44] F. Zhao and J. Tang, Phys. Rev. D **92**, 083011 (2015).
[45] F. Zhao, J. Tang, and F. He, Phys. Rev. D **93**, 123017 (2016).
[46] Z. Stuchlík and S. Hledík, Acta Phys. Slovaca **52**, 363 (2002), erratum notice can be found at http://www.physics.sk/aps/pubs/2002/aps-2002-52-5-363.pdf.
[47] Z. Stuchlík and P. Slaný, Phys. Rev. D **69**, 064001 (2004).
[48] G. V. Kraniotis, Classical Quantum Gravity **21**, 4743 (2004).
[49] G. V. Kraniotis, in *Dark matter in astro- and particle physics. Proceedings of the International Conference DARK 2004, College Station, TX, 2004*, edited by H. V. Klapdor-Kleingrothaus and R. Arnowitt (Springer, Berlin, 2005), p. 469.
[50] G. V. Kraniotis, Classical Quantum Gravity **24**, 1775 (2007).
[51] N. Cruz, M. Olivares, and J. R. Villanueva, Classical Quantum Gravity **22**, 1167 (2005).
[52] V. Kagramanova, J. Kunz, and C. Lammerzahl, Phys. Lett. B **634**, 465 (2006).
[53] A. N. Aliev, Phys. Rev. D **75**, 084041 (2007).
[54] J.-H. Chen and Y.-J. Wang, Chin. Phys. B **17**, 1184 (2008).
[55] L. Iorio, New Astron. **14**, 196 (2009).
[56] E. Hackmann, B. Hartmann, C. Lämmerzahl, and P. Sirimachan, Phys. Rev. D **82**, 044024 (2010).
[57] M. Olivares, J. Saavedra, C. Leiva, and J. R. Villanueva, Mod. Phys. Lett. A **26**, 2923 (2011).
[58] P.-H. Chavanis and T. Harko, Phys. Rev. D **86**, 064011 (2012).
[59] B. Chauvineau and T. Regimbau, Phys. Rev. D **85**, 067302 (2012).
[60] L. Zou, F.-Y. Li, and T. Li, Int. J. Mod. Phys. D **23**, 1450016 (2014).
[61] T. Sarkar, S. Ghosh, and A. Bhadra, Phys. Rev. D **90**, 063008 (2014).
[62] P. A. González, M. Olivares, and Y. Vásquez, Eur. Phys. J. C **75**, 464 (2015).
[63] A. Maciel, D. C. Guariento, and C. Molina, Phys. Rev. D **91**, 084043 (2015).
[64] D. Kunst, V. Perlick, and C. Lämmerzahl, Phys. Rev. D **92**, 024029 (2015).
[65] A. F. Zakharov, J. Astrophys. Astron. **36**, 0 (2015).
[66] I. Arraut, Int. J. Mod. Phys. D **24**, 1550022 (2015).
[67] I. Arraut, Europhys. Lett. **109**, 10002 (2015).
[68] C. A. Sporea and A. Borowiec, Int. J. Mod. Phys. D **25**, 1650043 (2016).
[69] T. Jacobson and T. P. Sotiriou, Phys. Rev. D **79**, 065029 (2009).
[70] M. Kološ and Z. Stuchlík, Phys. Rev. D **82**, 125012 (2010).
[71] Z. Gu and H. Cheng, Gen. Relativ. Gravit. **39**, 1 (2007).
[72] L. Wang and H. Cheng, Phys. Lett. B **713**, 59 (2012).
[73] Z. Stuchlík and M. Kološ, Phys. Rev. D **85**, 065022 (2012).
[74] Z. Stuchlík and M. Kološ, J. Cosmol. Astropart. Phys. 10 (2012) 008.
[75] Z. Stuchlík and M. Kološ, Phys. Rev. D **89**, 065007 (2014).
[76] A. Müller and B. Aschenbach, Classical Quantum Gravity **24**, 2637 (2007).
[77] P. Slaný and Z. Stuchlík, Classical Quantum Gravity **25**, 038001 (2008).
[78] Z. Stuchlík, P. Slaný, and S. Hledík, Astron. Astrophys. **363**, 425 (2000).
[79] P. Slaný and Z. Stuchlík, Classical Quantum Gravity **22**, 3623 (2005).
[80] L. Rezzolla, O. Zanotti, and J. A. Font, Astron. Astrophys. **412**, 603 (2003).
[81] B. Aschenbach, Chin. J. Astron. Astrophys. **8**, 291 (2008); in 7th International Workshop on Multifrequency Behaviour of High Energy Cosmic Sources, Vulcano, Italy, 2007 (unpublished).
[82] Z. Stuchlík, P. Slaný, G. Török, and M. A. Abramowicz, Phys. Rev. D **71**, 024037 (2005).
[83] H. Kučáková, P. Slaný, and Z. Stuchlík, J. Cosmol. Astropart. Phys. 01 (2011) 033.

[84] D. Perez, G. E. Romero, and S. E. Perez Bergliaffa, Astron. Astrophys. **551**, A4 (2013).
[85] S. Chakraborty, Classical Quantum Gravity **32**, 075007 (2015).
[86] D. Pugliese and Z. Stuchlík, Astrophys. J. Suppl. Ser. **221**, 25 (2015).
[87] D. Pugliese and Z. Stuchlík, Astrophys. J. Suppl. Ser. **223**, 27 (2016).
[88] J. Karkowski and E. Malec, Phys. Rev. D **87**, 044007 (2013).
[89] P. Mach and E. Malec, Phys. Rev. D **88**, 084055 (2013).
[90] P. Mach, E. Malec, and J. Karkowski, Phys. Rev. D **88**, 084056 (2013).
[91] P. Mach, Phys. Rev. D **91**, 084016 (2015).
[92] F. Ficek, Classical Quantum Gravity **32**, 235008 (2015).
[93] Z. Stuchlík and J. Kovář, Int. J. Mod. Phys. D **17**, 2089 (2008).
[94] Z. Stuchlík, P. Slaný, and J. Kovář, Classical Quantum Gravity **26**, 215013 (2009).
[95] Z. Stuchlík and J. Schee, J. Cosmol. Astropart. Phys. 09 (2011) 018.
[96] J. Schee, Z. Stuchlík, and M. Petrásek, J. Cosmol. Astropart. Phys. 12 (2013) 026.
[97] Z. Stuchlík and J. Schee, Int. J. Mod. Phys. D **21**, 1250031 (2012).
[98] E. G. Gimon and P. Hořava, arXiv:hep-th/0405019v1.
[99] E. K. Boyda, S. Ganguli, P. Hořava, and U. Varadarajan, Phys. Rev. D **67**, 106003 (2003).
[100] E. G. Gimon and P. Hořava, Phys. Lett. B **672**, 299 (2009).
[101] Z. Stuchlík and J. Schee, Classical Quantum Gravity **29**, 065002 (2012).
[102] F. de Felice, Astron. Astrophys. **34**, 15 (1974).
[103] C. T. Cunningham, Astrophys. J. **202**, 788 (1975).
[104] F. de Felice, Nature (London) **273**, 429 (1978).
[105] Z. Stuchlík, Bull. Astron. Inst. Czech. **31**, 129 (1980).
[106] Z. Stuchlík, S. Hledík, and K. Truparová, Classical Quantum Gravity **28**, 155017 (2011).
[107] K. Hioki and K.-i. Maeda, Phys. Rev. D **80**, 024042 (2009).
[108] Z. Stuchlík and J. Schee, Classical Quantum Gravity **27**, 215017 (2010).
[109] Z. Stuchlík and J. Schee, Classical Quantum Gravity **29**, 025008 (2012).
[110] Z. Stuchlík and J. Schee, Classical Quantum Gravity **30**, 075012 (2013).
[111] A. Bosma, Astron. J. **86**, 1791 (1981).
[112] V. C. Rubin, in *Comparative HI Content of Normal Galaxies, Proceedings of the Workshop, Green Bank, West Virginia, 1982*, edited by M. Haynes and R. Giovanelli (National Radio Astronomy Observatory, Charlottesville, 1982), p. 42.
[113] J. Binney and S. Tremaine, *Galactic Dynamics*, Princeton Series in Astrophysics (Princeton University Press, Princeton, NJ, 1988), p. 755.
[114] L. Iorio, Mon. Not. R. Astron. Soc. **401**, 2012 (2010).
[115] J. F. Navarro, C. S. Frenk, and S. D. M. White, Astrophys. J. **490**, 493 (1997).
[116] C. Cremaschini and Z. Stuchlík, Int. J. Mod. Phys. D **22**, 1350077 (2013).
[117] S. Weinberg, *Cosmology*, 1st ed. (Oxford University Press, New York, 2008), p. 544.
[118] R. F. Tooper, Astrophys. J. **140**, 434 (1964).
[119] G. Börner, *The Early Universe* (Springer-Verlag, Berlin, 1993).
[120] E. W. Kolb and M. S. Turner, *The Early Universe* (Addison-Wesley, Redwood City, CA, 1990).
[121] S. L. Shapiro and S. A. Teukolsky, *Black Holes, White Dwarfs and Neutron Stars: The Physics of Compact Objects* (Wiley, New York, 1983), p. 672.
[122] Z. Stuchlík, S. Hledík, J. Šoltés, and E. Østgaard, Phys. Rev. D **64**, 044004 (2001).
[123] U. S. Nilsson and C. Uggla, Ann. Phys. **286**, 292 (2000).
[124] C. G. Böhmer and G. Fodor, Phys. Rev. D **77**, 064008 (2008).
[125] M. A. Abramowicz, Mon. Not. R. Astron. Soc. **245**, 733 (1990).
[126] Z. Stuchlík, S. Hledík, and J. Juráň, Classical Quantum Gravity **17**, 2691 (2000).
[127] J. Hladík and Z. Stuchlík, J. Cosmol. Astropart. Phys. 07 (2011) 012.
[128] J. Ziolkowski, Chin. J. Astron. Astrophys. **8**, 273 (2008); 7th International Workshop on Multifrequency Behaviour of High Energy Cosmic Sources, Vulcano, Italy, 2007 (unpublished).
[129] I. Arraut, Mod. Phys. Lett. A **28** (2013).
[130] I. Arraut, Phys. Rev. D **90**, 124082 (2014).
[131] L. D. Landau and E. M. Lifshitz, *Fluid Mechanics* (Pergamon, New York, 1987).
[132] M. A. Abramowicz, B. Carter, and J. Lasota, Gen. Relativ. Gravit. **20**, 1173 (1988).
[133] M. A. Abramowicz, J. C. Miller, and Z. Stuchlík, Phys. Rev. D **47**, 1440 (1993).
[134] J. Kovář and Z. Stuchlík, Classical Quantum Gravity **24**, 565 (2007).
[135] O. Semerák, Nuovo Cimento B **110**, 973 (1995).
[136] S. Hledík, *Gravitation: Following the Prague Inspiration (A Volume in Celebration of the 60th Birthday of Jiří Bičák)*, edited by O. Semerák, J. Podolský, and M. Žofka (World Scientific, Singapore, 2002), p. 161.
[137] Z. Stuchlík, J. Hladík, M. Urbanec, and G. Török, Gen. Relativ. Gravit. **44**, 1393 (2012).
[138] M. A. Abramowicz, P. Nurowski, and N. Wex, Classical Quantum Gravity **12**, 1467 (1995).
[139] C. G. Böhmer, Gen. Relativ. Quantum **36**, 1039 (2004).
[140] Z. Stuchlík, G. Török, S. Hledík, and M. Urbanec, Classical Quantum Gravity **26**, 035003 (2009).
[141] U. S. Nilsson and C. Uggla, Ann. Phys. (N.Y.) **286**, 292 (2000).
[142] V. Faraoni, M. Lapierre-Léonard, and A. Prain, J. Cosmol. Astropart. Phys. 10 (2015) 013.
[143] V. Faraoni, Phys. Dark Univ. **11**, 11 (2016).
[144] J. Ziolkowski, Mon. Not. R. Astron. Soc. **358**, 851 (2005).
[145] J. Ziolkowski, Nuovo Cimento Soc. Ital. Fis. **120B**, 757 (2005); Vulcano Workshop 2004 on Frontier Objects in Astrophysics, Vulcano, Italy, 2004 (unpublished).
[146] A. Linde, New Sci. **105**, 14 (1985).

[147] T. Boeckel and J. Schaffner-Bielich, Phys. Rev. Lett. **105**, 041301 (2010).
[148] T. Boeckel and J. Schaffner-Bielich, Phys. Rev. D **85**, 103506 (2012).
[149] Z. Stuchlík and S. Hledík, in *Proceedings of RAGtime 6/7: Workshops on Black Holes and Neutron Stars, Opava, Czech Republic, 2005*, edited by S. Hledík and Z. Stuchlík (Silesian University in Opava, Opava, 2005), p. 209.
[150] C. G. Böhmer and T. Harko, Phys. Rev. D **71**, 084026 (2005).
[151] R. F. Tooper, Astrophys. J. **142**, 1541 (1965).